

Journal Pre-proofs

Tubulin Inhibitors: Discovery of a New Scaffold Targeting Extra-binding Residues within the Colchicine Site through Anchoring Substituents Properly Adapted to their Pocket by a Semi-flexible Linker

Raed M. Maklad, El-Shimaa M.N. AbdelHafez, Dalia Abdelhamid, Omar M. Aly

PII: S0045-2068(19)31218-0
DOI: <https://doi.org/10.1016/j.bioorg.2020.103767>
Reference: YBIOO 103767

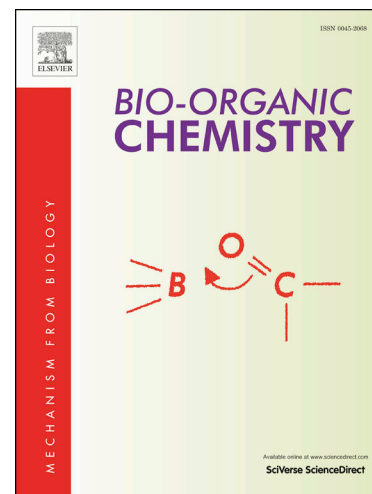
To appear in: *Bioorganic Chemistry*

Received Date: 28 July 2019
Revised Date: 6 March 2020
Accepted Date: 15 March 2020

Please cite this article as: R.M. Maklad, E.M.N. AbdelHafez, D. Abdelhamid, O.M. Aly, Tubulin Inhibitors: Discovery of a New Scaffold Targeting Extra-binding Residues within the Colchicine Site through Anchoring Substituents Properly Adapted to their Pocket by a Semi-flexible Linker, *Bioorganic Chemistry* (2020), doi: <https://doi.org/10.1016/j.bioorg.2020.103767>

This is a PDF file of an article that has undergone enhancements after acceptance, such as the addition of a cover page and metadata, and formatting for readability, but it is not yet the definitive version of record. This version will undergo additional copyediting, typesetting and review before it is published in its final form, but we are providing this version to give early visibility of the article. Please note that, during the production process, errors may be discovered which could affect the content, and all legal disclaimers that apply to the journal pertain.

© 2020 Published by Elsevier Inc.



Tubulin Inhibitors: Discovery of a New Scaffold Targeting Extra-binding Residues within the Colchicine Site through Anchoring Substituents Properly Adapted to their Pocket by a Semi-flexible Linker

Raed M. Maklad ^{a,b,c,*}, El-Shimaa M. N. AbdelHafez ^d, Dalia Abdelhamid ^d, Omar M. Aly ^d

^a Institute of Drug Discovery and Development, Kafrelsheikh University, Kafrelsheikh, Egypt.

^b Pharmaceutical Chemistry Department, Faculty of Pharmacy, Kafrelsheikh University, Kafrelsheikh 33516, Egypt.

^c Zewail City of Science and Technology, 6th of October, Giza, Egypt.

^d Medicinal Chemistry Department, Faculty of Pharmacy, Minia University, Minia, Egypt.

* Corresponding author:

Raed M. Maklad

Pharmaceutical Chemistry Department, Faculty of Pharmacy,
Kafrelsheikh University, Kafrelsheikh 33516, Egypt

E-mail address: raed_mostafa2010@yahoo.com; rmostafa@zewailcity.edu.eg

Abstract

Bis-hydrazides **13a-h** were designed and synthesized as potential tubulin inhibitors selectively targeting the colchicine site between α - and β -tubulin subunits. The newly designed ring-B substituents were assisted at their ends by ‘anchor groups’ which are expected to exert binding interaction(s) with new additional amino acid residues in the colchicine site (beyond those amino acids previously reported to interact with reference inhibitors as CA-4 and colchicine). Conformational flexibility of *bis*-hydrazide linker assisted these ‘extra-binding’ properties through relieving ligands’ strains in the final ligand-receptor complexes. Compound **13f** displayed the most promising computational and biological study results in the series: MM/GBSA binding energy of -62.362 kcal/mol (extra-binding to Arg α :221, Thr β :353 & Lys β :254); 34% NCI-H522 cells’ death (at 10 μ M), IC₅₀= 0.073 μ M (MTT assay); significant cell cycle arrest at G2/M phase; 11.6% preG1 apoptosis induction and 83.1% *in vitro* tubulin inhibition (at concentration = IC₅₀). Future researchers in *bis*-hydrazide tubulin inhibitors are advised to consider the 2-chloro-*N*-(4-substituted-phenyl)acetamide derivatives as compound **13f** due to extra-binding properties of their ring B.

Keywords: Antiproliferative agent; Anticancer; Hydrazide; Tubulin inhibitor; Combretastatin A-4 analog; Molecular modeling; Colchicine binding site; Docking; Drug design; In silico study.

1. Introduction

Tubulin targeting agents [1–9] were historically classified [10,11] according to their binding sites within tubulin protein [4,12–21]. Owing to their structure simplicity, colchicine-binding site (CBS) inhibitors [17] especially combretastatin A-4 (CA-4) derivatives were subjected to full SAR study [22–25] (**Fig. 1** “Supplementary Material”). Several reported experimental results proved that the 3,4,5-trimethoxyaryl ring (ring A) of CA-4 (**1**) and its analogues is essential for the activity [26,27] while ring B has been amenable to modifications [22–25] (**Fig. 1**), especially at C3' and C4'. The C3'-substituted analogues with hydrogen bond acceptors (HBAs) e.g. Cl atom (compounds **2f,g** [28]), NH₂ group (compound **3** [24]) and OH group (compounds **1** [29], **4** [30] and **6a,b** [31]) displayed the highest biological activities. Meanwhile, OMe and OEt groups [26,28] remained the most common C4'-substitutions which preserve the activity of the parent nucleus. Higher sterically-hindered alkyl substitution usually leads to loss of activity [26,28]. Regarding the olefinic linker, *cis*-geometry was necessary for maximal activity [26]. Accordingly, *cis*-restricted heterocyclic linkers were reported [32–35], tetrazole analogues **2a-g** [28] (**Fig. 1**) serve a representative example. However, open-chain linker analogues (ranging from one- to four-atom length) [24,30,31,36] also preserved the activity (compounds **2-6**, **Fig. 1**).

Target compounds (**13a-h**) were designed so as to preserve the general structural features of the CBS tubulin inhibitors (**Fig. 1** “Supplementary Material”) while introducing a new linker as well as a new para-substitution pattern for the ring B. Designing new linkers have been relatively encouraged so as to overcome some specific possible limitations concerning the classical *cis*-olefinic linker. The liability to metabolic isomerization to the *trans*-isomer was reported as a possible metabolic pathway of CA-4 in rat and human liver microsomes [37]. Moreover, the linker chain stereochemistry played an interesting role. It is believed that the linker may not be involved into interaction with the receptor. However, it preserves an optimum mean dihedral angle between both aromatic rings (for maximal receptor interaction) beyond which narrow range of deviation is allowed. Thus, if an open-chain linker was introduced with limited conformational changes, an optimum receptor fitting and higher activity may be reached. For example, the (1*Z*,3*E*)-isomer of the conjugated diene analogue **5** [36] and the (*E*)-isomer of the chalcone analogue **6** [31] displayed optimal activities among all possible geometrical isomers. Compound **5b** (**Fig. 1**) has a conjugated diene linker with an inner C2-C3 single bond which allows, to some extent, free rotation. Similarly, compound **6b** (**Fig. 1**) has some free rotation

around the inner C-C single bond of the α,β -unsaturated ketone linker. Despite this partial flexibility of the linker, both compounds were potent. Thus, complete rigidity of the linker was not a must. The design of the linker chain in compounds (**13a-h**) was based on preserving some structural rigidity of the lead (CA-4), and some similar flexibility to that of compounds **5b** and **6b**, at the same time. Both rigidity and flexibility are expected to be maintained in balance by the effect of resonance as well as free N-N single bond rotation, respectively (for more discussion, see section **3.1.1**).

Fig. 1. Comparative cytotoxicity and antitubulin activity study of CA-4 (**1**) [24,28,29,31,36] against some of its reported potent analogues (**2** [28], **3** [24], **4** [30], **5** [36] and **6** [31]).

Formerly, similar linker chains like *N*-acylhydrazones [38,39] were versatile in several drugs. Regarding the anticancer drug design, several structurally-related linker chains were designed in potential antiproliferative agents; hydrazone [40,41], hydrazide-hydrazone [42–50], *bis*-hydrazide [45,51–53], ketohydrazide-hydrazone [54], ketoamide [55], thiosemicarbazone [42] and aroylhydrazone [49] were all reported examples of possible open-chain linker functionalities. Regarding the *bis*-hydrazide scaffold, it was more frequently reported as a possible intermediate for the synthesis of heterocyclic pharmaceutical agents [56–60]. Meanwhile, only a few studies (to the best of our knowledge) have targeted the design of potent antiproliferative anti-tubulin agents having *bis*-hydrazide linkers [45,51,53] or linkers which are structurally-related to *bis*-hydrazide [54,55,61].

The little number of research articles covering this point, as well as the large number of those discussing anticancer drug candidates structurally-related to *bis*-hydrazide scaffold [38–55] have increased our curiosity about the expected biological activity of the new scaffold. In addition, the narrow range of studied ring-B *para*-substituents [26,28] has created our motivation to optimize C4'-substituent chain length with incorporation of new terminal groups. Varying the degrees of electronic and/or hydrophobic parameters of these C4'-substituents was utilized as a helpful technique for finding an extra-binding site within the receptor pocket (section **3.1**. provides more details about the design of target *bis*-hydrazides **13a-h** as potential tubulin binding agents).

2. Results:

2.1. Molecular Modeling (*In Silico*) Study:

2.1.1. Receptor-based Pharmacophore Hypothesis:

Since the exact X-ray structure of tubulin was frequently reported with several co-crystallized ligands [62–67], we utilized Phase [68] to generate a receptor-based pharmacophore hypothesis. After, a PDB survey since 2004 to present, all the reported PDB files of tubulin co-crystallized with ligands inside the CBS were downloaded. They are listed as follows: 1SA0 [62], 1SA1 [62], 4O2B [64], 5GON [65], 5JVD [66], 5LP6 [63] and 5LYJ [67]. Then, all the ligand-receptor interactions were defined and used directly to generate a 15-feature pharmacophore (**Fig. 2A**). After ligand-pharmacophore alignment, a validation step was performed *via* calculation of "Phase Screen Score" for reference and target compounds. Among the series **13a-h**, compounds **13a**, **13g** and **13f** displayed the best fitting (**Fig. 2B**), giving "Phase Screen Score" values of 0.58, 0.54 and 0.60, respectively. Interestingly, both compounds **13a** & **13f** displayed protrusion of the 4'-substitution outside the pharmacophore (**Fig. 2B**). Can the C=C and/or the NHCOCH₂Cl groups (in compounds **13a** & **13f**, respectively) target different amino acid residue(s) within the CBS other than those interacting with reference co-crystallized tubulin ligands [62–67] (**Fig. 2**)?? Section 3.1.2 serves potential answers to this question.

Fig. 2. A) Proposed receptor-based pharmacophore hypothesis having 15 features: Hydrophobic (Hp) interactions (in green); hydrogen bond acceptor (HBA) interactions (in red); hydrogen bond donor (HBD) interactions (in blue). Close receptor amino acid residues (wire representation) are colored by atom (C: grey, N: blue, O: red). Amino acid labels (Cys 241, Asn 258, Thr 179 ...) are shown in blue. Feature-feature distances are represented as dashed lines in yellow and their values (in angstrom) are shown in yellow. B) Ligand alignments of compounds **13a**, **13f** and **13g** (atom style: thick-tube representation; color {by atom: C: grey, H: white, N: blue, O: red, Cl: green}) to the proposed Pharmacophore: H-bond (dashed line in yellow); π -cation interaction (dashed line in blue).

2.1.2. Docking Study, Post-docking Energy Minimization & Scoring:

Docking study of target compounds **13a-h** inside the CBS of tubulin (PDB code 1SA0) [62] was carried out using Maestro 9.0 (Maestro, version 9.0 Schrödinger, LLC, New York, USA, 2009. www.schrodinger.com). The results revealed superior "docking scores" for compounds **13b**, **13d**, **13f** and **13h** (-6.454, -6.409, -5.935 and -5.835, respectively) against colchicine (-5.008) and higher than or comparable to CA-4 (-6.062). This represents a rough measure of the affinity of the ligand to the rigid receptor. However, more reliable results were obtained after refinement of the overall ligand-receptor complex using Prime [70]. Now, minimization of ligand strain was considered, with respect to several acceptable low energy receptor conformations

(based on the Induced-fit theory by Daniel Koshland in 1958 [71]). Finally, an accurate MM/GBSA (Molecular Mechanics/Generalized Born Surface Area) energy scoring function was employed to evaluate the ligand strain and the binding interactions in the final refined receptor-ligand complex.

Fig. 3. Docking study of top three compounds **13f**, **13e** and **13h** inside CBS of tubulin.

The detailed docking results including the receptor interactions (amino acid residue, type, length, per-residue score and clashes) as well as the ligand strain energy, the docking score and the MM/GBSA binding energy of all target compounds *vs.* colchicine and CA-4 in addition to the detailed procedure are found in the “Supplementary Material”.

Among the series **13a-h**, compound **13f** displayed the highest binding energy (-62.362 kcal/mol). This recommends compound **13f** as the most efficient ligand in the series, with eight H-bonding interactions with the receptor and one hydrophobic one (**Fig. 3**). The most important amino acid is Thr β :353 (per-residue score= -8.019) due to the formation of two H-bonds of 1.73 and 2.09 Å length. The 4-chloroacetamido group is involved into three H-bonding interactions with Lys β :254, Cys β :241 & Leu β :252 and one hydrophobic one with Leu β :255.

Compounds **13e** & **13h** displayed considerably high values of binding energy (-61.072 and -59.947 kcal/mol, respectively), as well. Furthermore, the 4-azidoacetamido group in compound **13h** displayed one H-bond with Tyr α :210 (1.82 Å) and another one with Gln α :176 (1.88 Å) as well as an additional H-bond with Leu β :252 (2.58 Å) in addition to other multiple hydrophobic interactions as shown in **Fig. 3**.

2.2. Chemistry:

2.2.1. Synthesis of target compounds **13a-h**:

Scheme 1. Synthesis of *bis*-hydrazides **13a-h**^a

^aReagents and conditions: i) NaOH/Me₂SO₄, reflux 2 h, then NaOH, reflux 2 h, then HCl; ii) SOCl₂, reflux 2 h then NaOMe/ MeOH, stirring at r.t, 2 h; iii) NH₂NH₂·H₂O/EtOH, reflux, 48 h; iv) SOCl₂/benzene, reflux 2 h; v) TEA, DMF, stirring at r.t, 2 h; vi) Na₂CO₃(aq.), EtOH, stirring, 80 °C, 8 h; vii) NaN₃(aq.), DMF, stirring, 75°C, overnight.

Bis-hydrazides **13a-h** were prepared as illustrated in **Scheme 1**, and characterized using ¹H NMR, DEPT-Q ¹³C NMR and elemental analysis (see the “Supplementary Material” for more details). Firstly, compound **8** [72] was prepared starting from gallic acid (**7**) *via* Williamson's

ether synthesis. Then, the ester **9** [73] was prepared in high yield by activating the acid **8** with thionyl chloride [74] followed by methanolysis of the produced crude acid chloride. After that, the hydrazide **10** [73] was prepared by treatment of the ester **9** with hydrazine hydrate. Acyl chlorides **12a** [75], **12b** [76], **12c** [77,78], **12d** [79], **12e** and **12f** [80] were prepared from their corresponding carboxylic acids **11a** [81], **11b** [82,83], **11c** [84], **11d** [85], **11e** [86] & **11f** [80,87] *via* reaction with thionyl chloride [74]. Acylation of hydrazide **10** with crude acyl chlorides **12a-f** afforded *bis*-hydrazides **13a-f**, the procedure was previously reported [88,89]. Compounds **13g** and **13h** were prepared from compounds **13e** and **13f** *via* ester hydrolysis and S_N2 reaction with sodium azide, respectively.

Compound **13g** was previously reported [90], so only ¹H NMR (Supplementary Material) and elemental analysis for this compound (“Experimental” section) was found to be sufficient for structure confirmation.

2.3. Biological evaluation of anticancer activity:

2.3.1. *In vitro* NCI-60 cell line panel cytotoxicity assay:

According to the protocol of the drug evaluation branch of the National Cancer Institute (NCI), Bethesda, USA, compounds **13a** and **13d-h** were selected for *in vitro* NCI-60 cell line panel cytotoxicity assay. The detailed growth inhibition percent for these *bis*-hydrazides against the NCI-60 cell line panel is found in **Table 3** (Supplementary Material). As shown in **Fig. 4**, compound **13f** displayed comparable antiproliferative activity to colchicine [91] and sometimes even higher (as in U251 cells). The NCI results revealed also that compounds **13a** and **13h** (4'-substituted ring-B derivatives) exhibited moderate cytotoxic activity against the NCI-H522 cell line (growth inhibition percent of 34.23 and 39.51%, respectively). Additionally, compound **13a** displayed moderate growth inhibitory activity against A549/ATCC and UACC-257 cells (growth inhibition 31.94 and 37.61%, respectively). Similar results were observed for compound **13h** against UACC-257 cells (30.26% growth inhibition). These results appreciate the effect of 4-*O*-allyl and 4-NHCOCH₂N₃ substitutions of ring B.

Regarding the 3',4'-disubstituted-ring-B derivatives (**13d,e** and **13g**): in most cell lines, **13d** has higher activity than **13g**. Moreover, it seems from the NCI results (**Table 3**, Supplementary Material) that compound **13e** has higher activity than compound **13g** (“33.65 vs. 10.08%” as well as “32.64 vs. 6.41%” growth inhibition for T-47D and SNB-75 cells, respectively). For detailed comments on the NCI results as well as the overall experimental results, see the “Discussion and

Conclusion” section. Unfortunately, no one of the members of *bis*-hydrazide series **13a-h** was selected for further five-dose screening (at 1, 0.1, 0.01, 0.001 and 0.0001 μM) by the NCI, including the potent derivative **13f**. More information about the NCI compound selection criteria are found in the “Supplementary Material”.

Fig. 4. NCI results of *in vitro* growth inhibition percent of **13f** vs. colchicine [91] against the most sensitive cell lines at 10 μM .

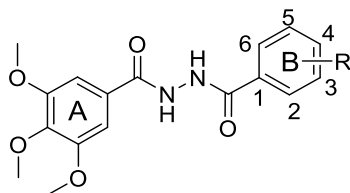
2.3.2. MTT assay:

To determinate their IC_{50} , all the synthesized *bis*-hydrazides **13a-h** were further analyzed using the MTT assay [92,93] against NCI-H522 cells, using CA-4 reference. The choice of this cell line was based on its high sensitivity to most tested *bis*-hydrazide derivatives in the NCI-60 cell line assay (**Fig. 4**). The results confirmed the promising activity of **13f** (IC_{50} = 0.073 μM vs. 0.001 μM for CA-4, see **Table 1**). Moderate activities of *bis*-hydrazides **13a**, **13c**, **13e** and **13g,h** were also observed (**Table 1**).

2.3.3. *In vitro* tubulin inhibitory activity assay:

In order to prove the mechanism of their antiproliferative activities, and confirm the validity of the molecular modeling results, *bis*-hydrazides **13a-h** were subjected to *in vitro* tubulin polymerization inhibitory activity assay against NCI-H522 cells using ELISA for β -tubulin (taking CA-4 as a positive control). The detailed results of tubulin assay are found in the “Supplementary Material”. The highest antitubulin activity was displayed by compound **13f** (83.1% inhibition), which intimately approaches the value of CA-4 (83.9%). Similarly, compounds **13h** and **13e** displayed remarkable antitubulin activities (73.9 & 73.3% inhibition, respectively as in **Table 1**).

Table 1. Calculated IC_{50} (μM) from linear equation of dose-response curve of compounds **13a-h** in MTT assay vs. their tubulin inhibition percent against NCI-H522 cells.

Diacylhydrazines **13a-h**

| Cpd | R= | MTT assay | | Tubulin assay | |
|-------------------|---|----------------------------|--|------------------------|----------------------------|
| | | Mean IC ₅₀ (μM) | Log IC ₅₀ ^a (μM) | Residual Tub Conc (μM) | Tub. Inhib. % ^b |
| 13a | 4-O-allyl | 31.72 | 1.50 ± 0.10 | 547.41 | 67.7 |
| 13b | 3-NO ₂ , 4-OCH ₃ | 55.41 | 1.74 ± 0.10 | 575.94 | 66.0 |
| 13c | 4-OCH ₃ | 38.61 | 1.59 ± 0.10 | 521.98 | 69.2 |
| 13d | 3-Cl, 4-OEt | 262.1 | 2.42 ± 0.07 | 652.86 | 61.5 |
| 13e | 3-OAc, 4-OCH ₃ | 20.16 | 1.30 ± 0.10 | 453.06 | 73.3 |
| 13f | 4-NHCOCH ₂ Cl | 0.073 | -1.14 ± 0.06 | 286.90 | 83.1 |
| 13g | 3-OH, 4-OCH ₃ | 31.91 | 1.50 ± 0.10 | 512.44 | 69.8 |
| 13h | 4-NH-CO-CH ₂ -N ₃ | 16.38 | 1.21 ± 0.10 | 442.56 | 73.9 |
| CA-4 (ref) | | 0.001 | -2.98 ± 0.04 | 273.36 | 83.9 |
| Control | | | | 1694.22 | |

^a Log IC₅₀: Log₁₀ concentration required to inhibit NCI-H522 cells' viability by 50% (mean ± SE from the dose-response curves of three experiments); ^b tubulin inhibition percent was calculated at concentration = IC₅₀ (from MTT assay) against the same cell line (NCI-H522).

2.3.4. Correlation between results of docking study and tubulin inhibitory activity assay:

To judge the significance of the docking study results, illustrated previously, the correlation between the computational study results (calculated binding energies) and the results of the anti-tubulin activity assay was studied. A graphical representation is represented in the "Supplementary Material, S39" correlating between the "-MM/GBSA dG Bind" and the "tubulin inhibition percent" of compounds **13a-h**. The plot shows a direct linear relationship with *r* (correlation coefficient) value of 0.904.

2.3.5. Cell cycle analysis by flow cytometry:

Furthermore, the most potent derivative (**13f**) was subjected to NCI-H522 cell cycle analysis *via* flow cytometry (Supplementary Material, S40) at 0.073 μM (the IC₅₀ value). The results

showed that compound **13f** produced a marked decrease in the cell population at G1 and S phases as compared to the control (**13f**: 45.13% and 15.45% *versus* control: 58.79% and 29.08%, respectively). Whereas, it caused significant increase of cell population in the G2/M phase compared to untreated control cells (39.42% *vs.* 12.13%, respectively). These results demonstrated that compound **13f** exerts its cytotoxic effect in NCI-H522 cells *via* arresting the cell growth in G2/M phase. Detailed results are provided in the “Supplementary Material”.

2.3.6. Annexin-V FITC apoptotic study:

Successful antiproliferative agents mostly have the ability to induce cancer cell apoptosis [94]. The annexin V apoptosis detection method is based on the observation that soon after initiating apoptosis, cells translocate the membrane phosphatidylserine (PS) from the inner face of the plasma membrane to the cell surface [95]. Once on the cell surface, PS can be easily detected by staining with a fluorescent conjugate of annexin V protein which has a high affinity for PS. Furthermore, the addition of Propidium Iodide (PI) stain (which cannot cross the membrane of live cells) facilitates the differentiation among necrotic, apoptotic and healthy cells [96]. Detection can be analyzed by flow cytometry which indicates whether the cell death is achieved through programmed apoptosis or nonspecific necrosis [97].

Therefore, the most active compound (**13f**) was subjected to “Annexin-V FITC” apoptotic study. The results displayed a marked increase in the percent of Annexin V-FITC positive apoptotic cells (including both the early and late apoptotic phases) from 0.73% to 11.61% (15.9 times increase compared to the untreated NCI-H522 cells (**Fig. 5**). Moreover, only 2.42% of the treated cells showed non-specific necrosis as compared to the control (0.68%). These findings propound undoubtedly that compound **13f** exhibits an apoptotic induction activity contributing to its mechanism of action as an antiproliferative agent.

Fig. 5. Representative dot plots of NCI-H522 cells treated with compound **13f** at its IC_{50} (0.073 μ M) for 24 h analyzed by flow cytometry after double cells’ staining with annexin-V FITC and PI. The blue color represents the stained Annexin V cells: a) results of control; b) results of **13f**.

3. Discussion and Conclusion:

3.1. Design of target *bis*-hydrazides **13a-h**:

3.1.1. Rationally-directed design:

As mentioned earlier in the “Introduction”, this study has been mainly devoted to the design of a proposed semi-flexible linker which maintains an optimum dihedral angle between both aromatic rings involved in receptor binding. The *bis*-hydrazide linker “CONHNHCO” is such an ideal one as it is capable of assuming narrow range of possible conformations inside the active site so that the molecule could adapt its structure easily to the receptor. Such conformational changes are brought about *via* free rotation around N-N single bond. Nevertheless, the conformation in *bis*-hydrazide scaffold is not completely free, due to C-N partial double bond character developed by resonance (**Fig. 6**) which restricts bond rotation to some extent. Again, this conformational restriction is also helpful in the design, as this maintains (to some extent) the rigidity of the *bis*-hydrazide linker chain (resembling the rigid olefinic linker in CA-4 which is a principle structural moiety in the SAR study). Four main possible conformers of the *bis*-hydrazide scaffold were proposed (**Fig. 6**) showing two possible resonating structures for each conformer. Hydrogen bonding may help assist the stability of a given conformer, thus contributing to structural rigidity. Reynolds et al [98] reported a theoretical basis for the study of the structure and the rotational barriers of diacylhydrazine conformations. For summary, the *bis*-hydrazide linker introduced in this work is expected to maintain balance between two useful structural features: a) rigidity (rotationally restricted C-N bond due to double bond character resulting from resonance); besides b) narrow range of conformational flexibility (due to N-N single bond free rotation). This balance allows facile adaptation of the *bis*-hydrazide structure to preserve an expected optimum distance between both substituted phenyl rings for maximal receptor binding.

Fig. 6: Four proposed conformational isomers for the *bis*-hydrazide scaffold.

Regarding the design of ring B substitution pattern: *bis*-hydrazides **13a**, **13f** & **13h** were substituted only at C4' while *bis*-hydrazides **13d**, **13e** & **13g** were substituted at C3' and C4'. Concerning the 3',4'-disubstituted analogues, common groups which preserve the activity as OMe [22–25] and OEt [23,25,28] were introduced. Similarly, the C3'-substituent was designed to maintain H-bond acceptors which again preserve the activity (**13g** was designed to retain the 3'-OH of CA-4 while **13d** preserves the 3'-Cl atom analogous to other potent reported 3'-Cl analogues [28,99]). Although it was previously reported that the 4'-*O*-acetyl substitution at the ring B leads to a remarkable decrease in the activity [22,25], the 3'-*O*-acetyl analogues are less frequent in the literature. Nevertheless, several *N*-acetyloxadiazoline analogues were reported to preserve the potency of the lead CA-4 [57,100,101]. One member of this series had the 3'-OAc-

4'-OMe phenyl as the ring B and still preserves the antiproliferative activity (even more active than the corresponding 4'-OMe phenyl analogue [101]). This result has created our motivation to discover the new role of the 3'-*O*-acetyl group in the *bis*-hydrazide series through designing compound **13e**. The corresponding 3'-OH derivative (**13g**) was designed to afford a reference for reliable comparison with **13e** (See the NCI-60 assay results in the "Supplementary Material"). Regarding compound **13b**, the 3'-NO₂ group was introduced to mimic some of the reported potent 3'-nitro-substituted CA-4 analogues [24,102].

Beyond this classical design, the 4'-substituted *bis*-hydrazides were subjected to major modification in their design. Firstly, compound **13c** was designed with the classical 4'-OMe group [22–25] as a standard *bis*-hydrazide derivative for comparison. Then, novel C4'-substituents (e.g. OCH₂CH=CH₂, NHCOCH₂Cl and NHCOCH₂N₃) were introduced in compounds **13a**, **13f** and **13h**, respectively. This was just a way of increasing the chain lengths of the C4'-substituents and assisting their free ends with anchor groups (as C=C, Cl and N₃, respectively) having different polarities, lipophilicities and steric effects (C=C is the most lipophilic, while N₃ is polar with negatively charged nitrogen and Cl quite polar and bulky).

Moreover, a literature survey was carried out to enhance this theoretical design by actually reported tubulin inhibitors containing similar anchor groups. The survey revealed some interesting examples of similarity e.g. the chloroacetyl derivatives of colchicine [103,104] as well as the *N*-chloroacetyl oxadiazole derivative reported elsewhere [57]. Although the latter was not subjected to biological evaluation, it was instead utilized as a synthetic precursor to the corresponding 2-acetoxyacetyl, 2-azidoacetyl, 2-(dimethylamino)acetyl derivatives which were all biologically active [57]. Among these compounds, the 2-azidoacetyl derivative displayed potent antiproliferative activity against HCT-15 & NCI-H460 cells (IC₅₀ in the nanomolar scale) [57]. Herein, the same 2-azidoacetyl group was introduced in compound **13h** in addition to its synthetic precursor "2-chloroacetyl group" in compound **13f**. Both functional groups were expected to act as H-bond acceptors targeting the close receptor amino acid residues. For reliable comparison, another poor H-bond acceptor group (preferably capable of hydrophobic binding) had better be designed in parallel. The 4'-allyloxy group in **13a** was thought to be sufficient. By that time, we had three new C-4' substituents at ring B in compounds **13a**, **13f** and **13h** designed to target an "extra-binding" site in the receptor pocket.

3.1.2. Computer-aided design:

As mentioned earlier (section **2.1.1.**), a pharmacophore hypothesis (**Fig. 2**) was generated from seven reported X-ray structures of tubulin individually co-crystallized with CBS ligands. Careful selection of the closest amino acid residues (3°A around each ligand) afforded the 13 amino acids showing 15 interaction features (10 Hp, 3 HBD and 2 HBA features, **Fig 3A**), which constitute the apparent shape of the receptor pocket. Nevertheless, other amino acid residues within the CBS (e.g. Tyr α :210, Arg α :221, Asp β :251...etc) haven't been targeted by reported ligand molecules. This may be due to strict adherence to the lead structure during the design of its analogues (e.g. compounds **2-6** in **Fig. 1** are so closely related to CA-4 that there is hardly any expected different binding interaction). However, beyond those 13 amino acids shown in **Fig. 2**, the “anchor groups” in this study (C=C, Cl and N₃ in compounds **13a**, **13f** and **13h**, respectively) have successfully targeted new amino acid residues within the CBS as shown by the following docking study results (**Table 1**, “Supplementary Material”): **13a** (extra-Van-der-Waals interaction of C=C with Asp β :251 [per-residue score -0.434]); **13f** (extra-H-bonding of Cl atom with Lys β :254 [2.25 $^{\circ}\text{A}$] in addition to other extra-H-bonding with Arg α :221 [2.34 $^{\circ}\text{A}$] and Thr β :353 [1.73 & 2.09 $^{\circ}\text{A}$] with per-residue scores of -3.947, -3.451 and -8.019, respectively); and **13h** (extra-H-bonding of N₃ group with Tyr α :210 [1.82 $^{\circ}\text{A}$] as well as other extra-H-bonding with Gln α :176 [1.88 $^{\circ}\text{A}$] and Leu β :252 [2.58 $^{\circ}\text{A}$] with per-residue scores of -0.22, -4.381 and -1.794, respectively), see detailed results in **Table 1** “Supplementary Material”. Generally, targeting new amino acid residue(s) (“*extra-binding*” site) within the CBS by the newly designed “anchor groups” usually adds further contribution to the binding energy (“*extra-binding*” properties). The final MM/GBSA scoring function has accurately ranked the series **13a-h** in terms of receptor binding energy and ligand strain. The best results were displayed by compound **13f** (MM/GBSA dG_{bind} -62.362 and ligand strain +3.949 kcal/mol, **Table 1** “Supplementary Material”).

3.2. Synthesis and biological evaluation of target compounds (13a-h):

3.2.1. Synthesis:

Chemical synthesis and characterization of target compounds **13a-h** was successfully carried out using simple and straightforward synthetic methodology (**Scheme 1**).

3.2.2. Antiproliferative activity studies:

The cytotoxicity investigation of *bis*-hydrazides **13a-h** passed into multiple stages. Firstly, the NCI-60 cell line panel SRB assay served a preliminary screening of cytotoxicity against wide

range of cancer cell lines derived from different types of cancer (leukemia, non-small cell lung cancer, breast cancer etc). The results of growth inhibition percent (measured at 10 μM concentration) of the NCI-60 cell line panel were interpreted so as to evaluate the series **13a-h** versus colchicine (reference data, 6-2016 [91], **Table 3** “Supplementary Material”). Similarly, the comparison in **Fig. 4** was held between the growth inhibition results of the most potent derivative **13f** and colchicine against the most sensitive cell line (which was NCI-H522 in our case). Unfortunately, none of compounds **13a-h** passed the selection criteria for the next step of five-dose assay including the most potent one **13f**. Thus, IC_{50} values had better be calculated by further multiple-dose cytotoxicity assay. Based on the results shown in **Table 3** and **Fig. 4**, we selected the NCI-H522 cell line for the next steps of biological evaluation. The MTT assay was considered the most common well-established technique available to us for cell viability measurement which can provide an accurate measure of cytotoxicity [92,93]. The new cell viability data obtained from the MTT assay were used in calculation of the dose-response curves for compounds **13a-h** and CA-4 against NCI-H522 cells, and then the IC_{50} values were calculated from the curves. **Table 1** provides a reliable comparison of the antiproliferative activities of compounds **13a-h** versus CA-4 in terms of their IC_{50} values against NCI-H522 cells.

The NCI-60 cell line panel assay as well as the MTT cytotoxicity assay revealed that compound **13f** displayed the maximal antiproliferative activity in the whole series (**Table 1**) and in some cell lines higher than colchicine (**Fig. 4**). This provided a potential proof of the previously illustrated extra-binding role of 4'- NHCOCH_2Cl group. Moderate activities of **13a** and **13h** against NCI-H522 confirmed the same hypothesis for 4'-allyloxy and 4'- $\text{NHCOCH}_2\text{N}_3$ groups, respectively. Regarding the 3',4'-disubstituted-ring-B derivatives; compound **13d** has a comparable to higher activity than **13g** against several cell lines especially HCT-116 and BT-549 (despite lower activity “ $\text{IC}_{50}=262.1\mu\text{M}$ ” against NCI-H522 cells, see **Table 1**). This enhances the recommendation of the 3'-Cl substituent as a better pharmacophoric moiety than the ordinary 3'-OH in this *bis*-hydrazide series. The promising results displayed by the previously reported 3'-chloro CA-4 analogues [28,99] enhance this proposal. Compound **13d** is expected to penetrate the cancer cell membrane more rapidly than **13g** due to higher log P and membrane dG insert values (more details are found in the "Supplementary Material"). Concerning compound **13e** (the 3'-*O*-acetyl derivative), it displayed higher activity when compared to **13g** (the corresponding 3'-OH derivative) as shown in SNB-75 and NCI-H522 cell lines (**Table 3**, Supplementary

Material). This provides a strong practical evidence to the theoretical docking study results of **13e** (acetyl group in **13e** exerts H-bonding with Cys β :241 (1.98 °A), as in **Fig. 3**). This may lead us to reevaluate the role of ester group in 3-*O*-acetyl CA-4 *bis*-hydrazide analogues as an extra-binding group when compared to the classical 3-OH group.

3.2.3. Insights into the mechanism of action of the most potent analogues:

Anti-tubulin activity proved the mechanism of action of this series especially compounds **13e**, **13f** and **13h**. Again **13f** was the most potent one (83.1% inhibition vs. 83.9% for CA-4). Linear relationship between anti-tubulin activity and the calculated binding energy in the “Supplementary Material” indicates the reliability of the docking results in *bis*-hydrazide derivatives. The linear equation can be used for rough prediction of the expected anti-tubulin activity of any proposed member of this series with different substitution pattern, *prior to* chemical synthesis.

Returning back to the most potent compound (**13f**), an additional insight into its mechanism of action was obtained from the results of NCI-H522 cell cycle analysis, which displayed cell growth arrest at the G2/M phase at the IC₅₀ value (0.073 μ M). Further contribution to the cytotoxicity of **13f** results from 11.61% apoptosis induction (15.9 times of control) at the preG1 phase with only 2.42% non-specific necrosis.

4. Experimental:

4.1. Chemistry

All substituted benzoic acids carboxylic acids **11a** [81], **11b** [82,83], **11c** [84], **11d** [85], **11e** [86] & **11f** [80,87], as well as gallic acid (**7**), the reagents and analytical or HPLC grade solvents were purchased from Sigma-Aldrich®. All melting points were determined on an electro-thermal melting point apparatus (Stuart Scientific, Model SMP1, U.K). Pre-coated silica gel plates (TLC aluminum sheets, silica gel 60 F₂₅₄, thickness 0.2 mm, Merck, Germany) were used. Visualization of the spots was effected by UV-lamp at $\lambda = 254$ nm. IR spectra were recorded on Nicolet IS5 FT-IR spectrometer. Unless otherwise stated, NMR spectrometric analysis was carried out in DMSO-*d*₆ solvent using Bruker Advance spectrometer (400 and 100 MHz for ¹H NMR and DEPT-Q ¹³C NMR experiments, respectively). Chemical shifts (δ) values are given in parts per million (ppm), relative to DMSO-*d*₆ (2.54 for proton and 40.45 ppm for carbon) and

coupling constants (J) in Hertz. Splitting patterns are designated as follows: s, singlet; d, doublet; t, triplet; q, quartet; dd, doublet of doublet; m, multiplet, brs; broad singlet. Elemental analysis was performed on Vario El Elementar CHN Elemental analyzer.

4.1.1. Preparation of 3,4,5-trimethoxybenzoic acid (**8**) [72]

The detailed procedure for preparation of this compound is included in the “Supplementary Material”. The identity of this compound was confirmed by its melting point 165–167°C (reported [72] 167-169°C). IR; 1681 cm^{-1} (C=O).

4.1.2. General procedure [74] for synthesis of substituted benzoyl chlorides

A mixture of the aromatic acid (2.500 mmol), thionyl chloride (0.894 g, 7.511 mmol) and benzene (7 mL) was refluxed for 3 h. Then, benzene and the excess of thionyl chloride were distilled off. The crude acid chloride was weighed by difference and used directly in the next step without any further purification. For further purification, recrystallization from hexane may be performed. Crude yields of acyl chlorides **12a** [75], **12b** [76], **12c** [77,78], **12d** [79], **12e** and **12f** [80] were as high as 70-95%.

4.1.3. Preparation of methyl 3,4,5-trimethoxybenzoate (**9**) [73]

The detailed procedure for preparation of compound (**9**) starting from 3,4,5-trimethoxybenzoyl chloride (prepared by the previously mentioned general method [74]) is included in the “Supplementary Material”. The identity of this compound was confirmed by its melting point 83°C (reported 82–83°C) [73] and by IR: 1717 cm^{-1} (C=O).

4.1.4. Preparation of 3,4,5-trimethoxybenzohydrazide (**10**) [73]

The detailed procedure for preparation of this compound is included in the “Supplementary Material”. The identity of this compound was confirmed by its melting point 166 °C (reported 168°C [73]). IR: 3323-3201 cm^{-1} (NHNH₂), 1702 cm^{-1} (C=O).

4.1.5. General procedure [88,89] for synthesis of bis-hydrazides **13a-f**

To a stirred solution of hydrazide (**10**) (2.002 mmol, 0.453 g) and triethylamine (2.283 mmol, 0.231 g) in DMF (15 mL), a solution of the appropriate acid chloride (2.100 mmol) in DMF (10 mL) was added dropwise. After stirring for 72 h at ambient temperature, the reaction

mixture was poured into 150 mL of ice water while vigorous stirring for 15 min. The precipitate was filtered under suction, washed several times with water, air-dried, then dried in the oven below 110°C for several hours, and finally recrystallized from hot saturated acetonitrile solution or (if insoluble in hot acetonitrile) washed with boiling ethyl acetate, then filtered and dried. In certain cases and whenever needed, the product may be further recrystallized to give the final *bis*-hydrazide. Theoretical yields percent were calculated for all derivatives as relative to compound **10**.

***N'*-(4-(Allyloxy)benzoyl)-3,4,5-trimethoxybenzohydrazide (13a)**

Yellowish white powder; (Yield: 0.707 g, 91%); m.p= 100-103°C; IR (neat): two broad bands 3426, 3195 cm⁻¹ (NHNH), 1669, 1654 cm⁻¹ (two C=O hydrazide); ¹H NMR (400 MHz, DMSO-*d*₆): δ 10.44 (1H, brs, NH), 10.40 (1H, brs, NH), 7.95 (2H, d, *J* = 8.9 Hz, ArH), 7.31 (2H, s, ArH), 7.11 (2H, d, *J* = 8.9 Hz, ArH), 6.10 (1H, ddt, *J*_{trans, cis, vic} = 17.2, 10.5, 5.3 Hz, olefinic H), 5.46 (1H, dd, *J*_{trans, gem} = 17.3, 1.5 Hz, olefinic H), 5.33 (1H, dd, *J*_{cis, gem} = 10.5, 1.3 Hz, olefinic H), 4.70 (2H, d, *J*_{vic} = 5.3 Hz, allylic CH₂), 3.89 (6H, s, 3,5-di(OCH₃)), 3.77 (3H, s, 4-OCH₃); ¹³C NMR (100 MHz, DMSO-*d*₆): δ 166.55, 166.42, 162.03, 153.75, 141.44, 134.32, 130.43, 128.71, 125.86, 118.89, 115.49, 106.02, 69.40, 61.20, 57.08. Anal. Calcd. for C₂₀H₂₂N₂O₆ (386.15): C, 62.17; H, 5.74; N, 7.25, Found: C, 62.39; H, 5.95; N, 7.12.

3,4,5-Trimethoxy-*N'*-(4-methoxy-3-nitrobenzoyl)benzohydrazide (13b)

Greenish white powder; (Yield: 0.619 g, 76%); m.p=118-120°C; IR (neat): two broad bands at 3223, 3003cm⁻¹ (NHNH), 1674, 1617 cm⁻¹ (two C=O hydrazide), 1489cm⁻¹ (NO₂); ¹H NMR (400 MHz, DMSO-*d*₆) δ 10.75 (1H, s, NH), 10.59 (1H, s, NH), 8.51 (1H, d, *J*_{meta} = 1.9 Hz, ArH), 8.29 (1H, dd, *J*_{ortho, meta} = 8.8, 1.9 Hz, ArH), 7.58 (1H, d, *J*_{ortho} = 8.9 Hz, ArH), 7.32 (2H, s, ArH), 4.06 (3H, s, 4-OCH₃ ring B), 3.89 (6H, s, 3,5-di(OCH₃) ring A), 3.77 (3H, s, 4-OCH₃ ring A); ¹³C NMR (100 MHz, DMSO-*d*₆) δ 166.20, 164.62, 155.58, 153.70, 141.47, 139.74, 134.57, 128.41, 125.47, 125.36, 115.58, 106.00, 61.11, 58.17, 57.02. Anal. Calcd. for C₁₈H₁₉N₃O₈ (405.12): C, 53.33; H, 4.72; N, 10.37, Found: C, 53.35; H, 4.79; N, 10.43.

***N'*-(4-methoxybenzoyl)-3,4,5-trimethoxybenzohydrazide (13c)**

Dark yellow powder; (Yield: 0.398 g, 55%); mp = 154-156°C; IR (neat) 1667,1651 cm⁻¹ (two C=O hydrazide); ¹H NMR (400 MHz, DMSO-*d*₆) δ 10.44 (1H, s, NH), 10.40 (1H, s, NH),

7.96 (2H, d, $J_{ortho} = 8.8$ Hz), 7.31 (2H, s, ArH), 7.10 (2H, d, $J_{ortho} = 8.8$ Hz), 3.89 (6H, s, 3,5-di(OCH₃)), 3.87 (3H, s, 4-OCH₃), 3.77 (3H, s, 4-OCH₃); ¹³C NMR (100 MHz, DMSO-*d*₆) δ 166.63, 166.49, 163.16, 153.79, 141.50, 130.49, 128.75, 125.78, 114.87, 106.09, 61.26, 57.14, 56.52. Anal. Calcd. For C₁₈H₂₀N₂O₆ (360.36): C, 59.99; H, 5.59; N, 7.77. Found: C, 60.25; H, 6.07; N, 7.82.

***N'*-(3-Chloro-4-ethoxybenzoyl)-3,4,5-trimethoxybenzohydrazide (13d)**

White powder (m.p = 177-181°C, yield = 0.393 g, 48%); IR (neat) 1670, 1650 cm⁻¹ (two C=O hydrazide); ¹H NMR (400 MHz, DMSO-*d*₆): δ 10.48 (2H, brs, NHNH), 8.04 (1H, d, $J_{meta} = 2.0$ Hz), 7.95 (1H, dd, $J_{ortho,meta} = 8.6, 2.0$ Hz), 7.32 (1H, d, $J_{ortho} = 8.8$ Hz), 7.30 (2H, s), 4.26 (2H, q, $J_{vic} = 6.9$ Hz, OCH₂CH₃), 3.89 (6H, s, 3,5-di(OCH₃)), 3.77 (3H, s, 4-OCH₃), 1.43 (3H, t, $J_{vic} = 7.0$ Hz, OCH₂CH₃). ¹³C NMR (100 MHz, DMSO-*d*₆): δ 166.13, 165.21, 157.50, 153.62, 141.36, 130.01, 129.03, 128.46, 126.20, 122.10, 114.20, 105.92, 65.64, 61.05, 56.96, 15.36. Anal. Calcd. For C₁₉H₂₁ClN₂O₆ (408.83): C, 57.59; H, 5.64; N, 11.19. Found: C, 57.60; H, 5.70; N, 11.23.

2-Methoxy-5-(2-(3,4,5-trimethoxybenzoyl)hydrazinecarbonyl)phenyl acetate (13e)

Brown powder, m.p = 135-138°C, yield: 0.385 g, 46%; ¹H NMR (400 MHz, DMSO-*d*₆): δ 10.46 (2H, brs, NHNH), 7.925 (1H, dd, $J_{ortho,meta} = 8.6, 2.0$ Hz), 7.71 (1H, d, $J_{meta} = 2.0$ Hz), 7.32 (1H, d, $J_{ortho} = 8.6$, ArH) overlapped with 7.30 (2H, s, ArH), 3.90 (3H, s, 4-OCH₃, ring B), 3.89 (6H, s, 3,5-di(OCH₃)), 3.77 (3H, s, 4-OCH₃, ring A), 2.34 (3H, s, CH₃C=O). ¹³C NMR (100 MHz, DMSO-*d*₆): δ 169.62, 166.31, 165.73, 154.85, 153.72, 141.46, 139.93, 128.57, 127.72, 125.79, 123.36, 113.49, 106.01, 61.16, 57.18, 57.05, 49.62, 21.36. Anal. Calcd. for C₂₀H₂₂N₂O₈ (418.40): C, 57.41; H, 5.30; N, 6.70. Found: C, 57.48; H, 5.70; N, 6.76.

2-Chloro-*N*-(4-(2-(3,4,5-trimethoxybenzoyl)hydrazinecarbonyl)phenyl)acetamide (13f)

Beyond the general methodology for synthesis of *bis*-hydrazides **13a-f** (in part 4.1.5), compound **13f** was further purified by several washings with boiling DCM, ethyl acetate and acetonitrile. Then, the remaining residue was loaded on a flash column using silica gel (80-120 mesh size) as stationary phase and a mixture of acetonitrile and methanol (1:1) as mobile phase. The appropriate fraction (having $R_f = 0.23$) was left undisturbed at ambient temperature to crystallize. The produced yellow crystals had m.p = 210-213°C (single spot on TLC). These crystals were used for the final NMR analysis without further purifications (Yield = 0.380 g, 45%). ¹H NMR (500 MHz, DMSO-*d*₆): δ 10.75 (1H, s, NH amide), 10.455, 10.453 (2H, two brs,

NHNH hydrazide), 7.95 (2H, d, $J_{ortho} = 8.5$ Hz), 7.76 (2H, d, $J_{ortho} = 8.8$ Hz), 7.30 (2H, s, ArH), 4.35 (2H, s, CH_2Cl), 3.88 (6H, s, 3,5-di(OCH₃)), 3.77 (3H, s, 4-OCH₃). ¹³C NMR (125 MHz, DMSO-*d*₆): δ 167.12, 166.18, 165.91, 153.63, 142.54, 141.37, 129.45, 128.57, 128.56, 119.68, 105.95, 61.06, 56.97, 44.54. Anal. Calcd. for C₁₉H₂₀ClN₃O₆ (421.83): C, 54.10; H, 4.78; N, 9.96. Found: C, 54.19; H, 4.83; N, 10.01.

4.1.6. Preparation of *N'*-(3-Hydroxy-4-methoxybenzoyl)-3,4,5-trimethoxybenzohydrazide (13g) [90]

Compound **13e** (99.2 mg, 0.237 mmol) was dissolved in 3 mL absolute ethanol, then added dropwise to a solution of sodium carbonate (0.053 g, 0.500 mmol) in 5 mL water. The mixture was heated while stirring at 80°C for 3 h, then solvent evaporated and the residue washed with water, filtered and finally recrystallized from acetonitrile to afford the final product as white crystals (m.p = 193-195°C); (Yield: 0.039 g, 44%); ¹H NMR (400 MHz, DMSO-*d*₆): δ 10.37 (1H, brs, NH), 10.30 (1H, brs, NH), 9.34 (1H, brs, OH), 7.45 (1H, dd, $J_{ortho,meta} = 8.4, 1.7$ Hz), 7.40 (1H, d, $J_{meta} = 1.8$ Hz), 7.30 (2H, s, ArH), 7.06 (1H, d, $J_{ortho} = 8.5$ Hz), 3.88 (6H, s, 3,5-di(OCH₃)), 3.88 (3H, s, 4-OCH₃), 3.77 (3H, s, 4-OCH₃). Anal. Calcd. for C₁₈H₂₀N₂O₇ (376.36): C, 57.44; H, 5.36; N, 7.44. Found: C, 57.49; H, 5.40; N, 7.45.

4.1.7. Preparation of 2-Azido-*N*-(4-(2-(3,4,5-trimethoxybenzoyl)hydrazinecarbonyl)phenyl) acetamide (13h)

A mixture of compound **13f** (0.100 g, 0.237 mmol), sodium azide (0.033 g, 0.508 mmol) and 5 mL DMF were heated while stirring at 75°C overnight and then poured into 30 mL water, filtered and finally recrystallized from acetonitrile to afford the final product as white crystals (m.p = 188-190°C; yield = 0.045 g, 44%); ¹H NMR (400 MHz, DMSO-*d*₆): δ 10.62 (1H, brs, NH), 10.48 (1H, brs, NH), 10.46 (1H, brs, NH), 7.94 (2H, d, $J_{ortho} = 8.5$ Hz), 7.77 (2H, d, $J_{ortho} = 8.4$ Hz), 7.29 (2H, s, ArH), 4.15 (2H, s, $\text{CH}_2\text{-N}_3$), 3.88 (6H, s, 3,5-di(OCH₃)), 3.76 (3H, s, 4-OCH₃). ¹³C NMR (100 MHz, DMSO-*d*₆): δ 168.12, 166.62, 166.59, 153.91, 142.70, 141.58, 129.71, 128.96, 128.94, 120.00, 109.82, 106.19, 61.40, 57.25, 52.57. Anal. Calcd. for C₁₉H₂₀N₆O₆ (428.14): C, 53.27; H, 4.71; N, 19.62. Found: C, 53.37; H, 4.79; N, 19.71.

4.2. Biological evaluation of anticancer activity:

4.2.1. NCI-60 cell line panel anticancer screening:

The NCI anticancer screening methodology has been described elsewhere in detail at https://dtp.cancer.gov/discovery_development/nci-60/methodology.htm. A summary of the experimental assay methodology is found in the “Supplementary Material”.

4.2.2. *In vitro* anti-proliferative activity using MTT assay: [92,93]

Cell culture:

NCI-H522 cancer cell lines were purchased from American Type Cell Culture Collection (ATCC, Manassas, USA) and grown on Dulbecco's modified Eagle's medium (DMEM) or Roswell Park Memorial Institute medium (RPMI 1640) supplemented with 100 mg/mL of streptomycin, 100 units/mL of penicillin, and 10% of heat-inactivated fetal bovine serum.

Measurement of cytotoxicity using MTT assay:

Cytotoxicity was determined through morphological changes in NCI-H522 cells treated with compounds **13a-h** in comparison with untreated control cells. Firstly, cells were grown as monolayer (10^4 cells/well in 96-well tissue culture plate) in media supplemented with 10% inactivated fetal bovine serum. Cells were incubated for 24 h at 37°C in a humidified incubator with 5% CO₂ before treatment to allow cells' attachment to the plate.

Then, NCI-H522 cells were treated individually with different concentrations (100 to 0.01 μM) of compounds **13a-h** & CA-4 (positive control). Eight wells were prepared for each concentration in addition to eight other wells without the test compounds as cell control. Cells were incubated with the tested compounds for 48 h into CO₂ incubator at 37°C and 5% CO₂. After 48 h, the control and treated cells were observed under inverted microscope (before completing the assay) for any morphology differences. Subsequently, culture media containing tested compound and dead cells were decanted leaving only viable attached cells into the plate. The plate was then washed twice with pre-warmed PBS (phosphate buffered saline). MTT reagent (40 μL) was added to each well including blank and negative control wells. After that, the plates were incubated in dark for 4 h for the reduction of MTT into formazan (purple needle color) by dehydrogenase activity in mitochondria of viable cells. DMSO (150 μL) was added to each well to solubilize the purple crystals of formazan. Finally, the absorbance was measured at 570 nm with microplate reader (ROBONIK TM P2000 Eliza plate reader).

The percentage of cell survival relative to control was calculated by the equation below:

$$\text{Survival Rate} = \frac{\text{As} - \text{Ab}}{\text{Ac} - \text{Ab}} \times 100\%$$

As Sample absorbance

Ac Control (NCI-H522 cells) absorbance

Ab Blank absorbance

The viability percent was plotted against the logarithm of sample concentration. Then the concentration that induces 50% of maximum inhibition of cell proliferation (IC₅₀) was calculated for each compound from their dose-response curves using Graph Pad Prism 7.00 software (Graph Pad software Inc, CA[®]).

4.2.3. *In vitro* tubulin polymerization inhibitory assay:

Cell culture:

NCI-H522 cancer cells were obtained from American Type Culture Collection, cells were cultured using DMEM (Invitrogen/Life Technologies) supplemented with 10% Fetal Bovine Serum (FBS) (Hyclone), 10 µg/mL of insulin (Sigma), and 1% penicillin-streptomycin. All of the other chemicals and reagents were from Sigma, or Invitrogen. Cells were plated (cells density 1.2–1.8 × 10,000 cells/well) in a volume of 100 µL complete growth medium + 100 µL of the tested compound per well in a 96-well plate for 18–24 h prior to β-tubulin assay.

NCI-H522 cells were lysed before the assay according to the following directions: Adherent cells were detached with trypsin and then collected by centrifugation (suspended cells can be collected by centrifugation directly). Cells were washed three times in cold PBS followed by resuspension again in PBS and finally ultrasonication 4 times. A final centrifugation at 1500 rpm for 10 min at 2–8 °C was needed to remove cellular debris.

Tubulin assay procedure:

In vitro anti-tubulin activities of compounds **13a-h** was measured using ELISA kit for β-tubulin (Cloud Clone. Corp.) on NCI-H522 cell line. Growing NCI-H522 cells were trypsinized, counted and seeded at the appropriate densities into 96-well microtiter plates. Cells then were incubated in a humidified atmosphere at 37°C for 24 h. The standards (NCI-H522 cell lysates containing untreated β-tubulin), the tested compounds, and the control (CA-4) were diluted to designated concentrations. On the 96-well microtiter plates 100 µL of each one of tested compounds, standard as well as control was added to each well, and incubated at 37°C for 2 h.

The solution was aspirated and 100 μL of prepared "Detection Reagent A" (biotin-conjugated anti- β -tubulin antibody) was added to each well. Incubation was done at 37°C for 2 h. After washing 100 μL of prepared Detection Reagent B (Avidin conjugated to HRP "Horseradish Peroxidase") was added and incubation was continued at 37 °C for 30 min. Five washings were done, then 90 μL of substrate solution of 3,3',5,5'-tetramethylbenzidine ("TMB", a chromogenic visualizing agent acting as a hydrogen donor for the reduction of liberated hydrogen peroxide by HRP) was added and incubated at 37 °C for 15-25 min. Stop solution (sulphuric acid) was added in 50 μL . Optical density (O.D.) of the reaction product (diimine of TMB) was measured at 450 nm using microplate reader (Spectromax Plus 96 well plate spectrophotometer). O.D. was measured for each compound at a concentration (μM) equaling the IC_{50} value of this compound against the same cell line (NCI-H522), in the previously mentioned MTT assay. A standard curve was plotted (using Graph Pad Prism 7.00 software, Graph Pad software Inc, CA[®]) which describes a relationship between blank-corrected optical density and the logarithm of tubulin concentration. The software was used to calculate the best-fit curve which was firstly used to restandardize the tubulin standards prepared by serial dilution. And then by interpolation, the curve was used to determine unknown logarithm of residual tubulin concentrations in cell lysates treated with known concentrations of samples (NCI-H522 cell lysates treated with compounds **13a-h**) and reference (NCI-H522 cell lysates treated with CA-4). Finally, tubulin inhibition percent was calculated relative to untreated control cells by the following equation:

$$\text{Tubulin Inhibition percent} = \frac{[\text{Tub}]_c - [\text{Tub}]_s}{[\text{Tub}]_c} \times 100\%$$

[Tub]_c Tubulin concentration in control NCI-H522 cells
[Tub]_s Residual tubulin concentration in treated (sample) cells

4.2.4. Cell cycle analysis:

The procedure was previously reported [105]. For summary, compound **13f** (at conc = IC_{50} = 0.073 μM) was incubated with NCI-H522 cells (2×10^5 cells/well) for 24 h. Then, cells were washed with ice-cold phosphate buffer saline (PBS) twice and then centrifuged. After that, cells were fixed in ethanol 70% (v/v) at 4 °C for 30 min. then washed again with PBS for another 30-min. period but now at 37 °C. Again, cells were collected by 2000-rpm centrifugation for 5 min., stained with propidium iodide (PI) buffer, gently and homogenously mixed, and left in darkness

at ambient temperature for 20 min. BD FACS CALIBER flow cytometer was used for analysis of DNA content of the cells.

4.2.5. Annexin-V FITC apoptotic study:

Generally, Annexin V-FITC/PI (fluorescein-isothiocyanate/propidium iodide) Apoptosis Detection Kit [ab#139418] (BioVision Research Products, 980 Linda Vista Avenue, Mountain View, CA 94043 USA) was used for apoptosis assay according to the manufacturer's instruction. Firstly, NCI-H522 cells (4×10^6 cells/well) were incubated with compound **13f** (at conc = IC_{50} = 0.073 μ M) for 24 h. Control experiment (with untreated NCI-H522 cells) was carried out for comparison. Cells were washed three times with ice-cold PBS, re-suspended in PBS and then stained for 15 min with 5 mL Annexin V-FITC and 5 mL PI binding buffer in dark place at ambient temperature. Finally, BD FACS CALIBER flow cytometer was used for analysis of stained cells and measurement of extent of apoptosis.

Acknowledgements

The IR spectroscopic analyses were funded by and carried out at the Faculty of Pharmacy, Minia University, Egypt. The authors acknowledge the National Cancer Institute, Bethesda, USA, for performing the *in vitro* single-dose NCI-60 cell line panel cytotoxicity assay. Acknowledgements are also extended to the Shanghai Key Laboratory of New Drug Design, School of Pharmacy, East China University of Science & Technology, Shanghai, China for providing access to the licensed software used in the molecular modeling studies. Deep thanks to Dr. Esam Rashwan, at Serum and Vaccine Research Institute, Dokki, Giza, Egypt for performing the cell cycle analysis, apoptotic study, MTT and tubulin assays. We acknowledge Dr. Ayman M. Ibrahim at Organic Chemistry Department, Faculty of Pharmacy, Deraya University, Minia, Egypt for appreciable efforts in the figures' editing. Unless otherwise stated, all chemical reagents, solvents, NMR analysis and biological studies were self-funded by the first author. Finally, the authors pay special thanks of gratitude to Dr. Minna M. Abdel-Fattah for her time and effort spent during revision of grammar and sentence structure in the whole manuscript.

Conflict of Interest

The authors declare that they have no conflict of interest.

Author Contributions

R.M. Maklad designed target compounds, carried out the molecular modeling studies, performed the chemical synthesis, literature survey, statistical analysis, data collection, analyzed the results wrote the manuscript. ES.M.N. AbdelHafez discussed the synthetic methodology, contacted NCI for cytotoxicity study, discussed biological results & revised the manuscript. D. Abdelhamid discussed the synthetic methodology, discussed the biological results, the conclusion & revised the manuscript. O.M. Aly put the research point (tubulin inhibitors), designed the biological evaluation tests, discussed the synthetic methodology & revised the manuscript.

Supplementary Material

SAR of CA-4 analogues; Synthetic methods for compounds **8-10**; Characterization of compounds **13a-h** using ^1H NMR, DEPT-Q ^{13}C NMR; detailed discussion on the docking study results and procedure; calculated log P and membrane permeability for compounds **13a-h**; NCI-60 cell line one-dose assay results of compounds **13a**, **13d-h** & colchicine; Principle of MTT assay; Correlation between results of antitubulin activity assay & docking study; Results of cell cycle analysis by flow cytometry; detailed results of cytotoxicity and ELISA anti-tubulin activity assays.

References:

- [1] D.M. Bollag, P.A. McQueney, J. Zhu, O. Hensens, L. Koupal, J. Liesch, M. Goetz, E. Lazarides, C.M. Woods, Epothilones, a new class of microtubule-stabilizing agents with a taxol-like mechanism of action, *Cancer Res.* 55 (1995) 2325–2333.
- [2] M. Harrison, C. Swanton, Epothilones and new analogues of the microtubule modulators in taxane-resistant disease, *Expert Opin. Investig. Drugs.* 17 (2008) 523–546. <https://doi.org/10.1517/13543784.17.4.523>
- [3] K.H. Altmann, B. Pfeiffer, S. Arseniyadis, B.A. Pratt, K.C. Nicolaou, The Chemistry and Biology of Epothilones—The Wheel Keeps Turning, *ChemMedChem.* 2 (2007) 396–423. <https://doi.org/10.1002/cmdc.200600206>.
- [4] R.M. Buey, I. Barasoain, E. Jackson, A. Meyer, P. Giannakakou, I. Paterson, S. Mooberry, J.M. Andreu, J.F. Díaz, Microtubule Interactions with Chemically Diverse Stabilizing Agents: Thermodynamics of Binding to the Paclitaxel Site Predicts Cytotoxicity, *Chem. Biol.* 12 (2005) 1269–1279. <https://doi.org/10.1016/j.chembiol.2005.09.010>.

- [5] R.L. Bai, G.R. Pettit, E. Hamel, Binding of dolastatin 10 to tubulin at a distinct site for peptide antimetabolic agents near the exchangeable nucleotide and vinca alkaloid sites, *J. Biol. Chem.* 265 (1990) 17141–17149.
- [6] A. Brossi, H.J.C. Yeh, M. Chrzanowska, J. Wolff, E. Hamel, C.M. Lin, F. Quin, M. Suffness, J. Silverton, Colchicine and its analogues: Recent findings, *Med. Res. Rev.* 8 (1988) 77–94. <https://doi.org/10.1002/med.2610080105>.
- [7] L.H. Zhang, L. Wu, H.K. Raymon, R.S. Chen, L. Corral, M.A. Shirley, R. Krishna Narla, J. Gamez, G.W. Muller, D.I. Stirling, J.B. Bartlett, P.H. Schafer, F. Payvandi, The Synthetic Compound CC-5079 Is a Potent Inhibitor of Tubulin Polymerization and Tumor Necrosis Factor- α Production with Antitumor Activity, *Cancer Res.* 66 (2006) 951–959. <https://doi.org/10.1158/0008-5472.CAN-05-2083>.
- [8] S.M. Kupchan, R.W. Britton, M.F. Ziegler, C.J. Gilmore, R.J. Restivo, R.F. Bryan, Tumor inhibitors. LXXXX. Steganacin and steganangin, novel antileukemic lignan lactones from *Steganotaenia araliacea*, *J. Am. Chem. Soc.* 95 (1973) 1335–1336. <https://doi.org/10.1021/ja00785a054>.
- [9] E. Hamel, Antimetabolic natural products and their interactions with tubulin, *Med. Res. Rev.* 16 (1996) 207–231.
- [10] T. Carlomagno, *Tubulin-Binding Agents*, Springer Berlin Heidelberg, Berlin, Heidelberg, 2009. <https://doi.org/10.1007/978-3-540-69039-9>.
- [11] S. Iwasaki, Antimetabolic agents: Chemistry and recognition of tubulin molecule, *Med. Res. Rev.* 13 (1993) 183–198. <https://doi.org/10.1002/med.2610130205>.
- [12] M. Zweifel, G.C. Jayson, N.S. Reed, R. Osborne, B. Hassan, J. Ledermann, G. Shreeves, L. Poupard, S.P. Lu, J. Balkissoon, D.J. Chaplin, G.J.S. Rustin, Phase II trial of combretastatin A4 phosphate, carboplatin, and paclitaxel in patients with platinum-resistant ovarian cancer, *Ann. Oncol.* 22 (2011) 2036–2041. <https://doi.org/10.1093/annonc/mdq708>.
- [13] K.A. Lyseng-Williamson, C. Fenton, Docetaxel: A Review of its Use in Metastatic Breast Cancer, *Drugs.* 65 (2005) 2513–2531. <https://doi.org/10.2165/00003495-200565170-00007>.
- [14] H.A. Burris, Single-agent docetaxel (Taxotere) in randomized phase III trials, *Semin. Oncol.* 26 (1999) 1–6.
- [15] R.L. Noble, The discovery of the vinca alkaloids--chemotherapeutic agents against cancer, *Biochem. Cell Biol. Biochim. Biol. Cell.* 68 (1990) 1344–1351.
- [16] B. Gigant, C. Wang, R.B.G. Ravelli, F. Roussi, M.O. Steinmetz, P.A. Curmi, A. Sobel, M. Knossow, Structural basis for the regulation of tubulin by vinblastine, *Nature.* 435 (2005) 519–522. [doi:10.1038/nature03566](https://doi.org/10.1038/nature03566).
- [17] Y. Lu, J. Chen, M. Xiao, W. Li, D.D. Miller, An Overview of Tubulin Inhibitors That Interact with the Colchicine Binding Site, *Pharm. Res.* 29 (2012) 2943–2971. [doi:10.1007/s11095-012-0828-z](https://doi.org/10.1007/s11095-012-0828-z).
- [18] T.J. Kim, M. Ravoori, C.N. Landen, A.A. Kamat, L.Y. Han, C. Lu, Y.G. Lin, W.M. Merritt, N. Jennings, W.A. Spannuth, R. Langley, D.M. Gershenson, R.L. Coleman, V. Kundra, A.K. Sood, Antitumor and Antivascular Effects of AVE8062 in Ovarian

- Carcinoma, *Cancer Res.* 67 (2007) 9337–9345. <https://doi.org/10.1158/0008-5472.CAN-06-4018>.
- [19] L. Bohlin, B. Rosen, Podophyllotoxin derivatives: drug discovery and development, *Drug Discov. Today*. 1 (1996) 343–351. [https://doi.org/10.1016/1359-6446\(96\)10028-3](https://doi.org/10.1016/1359-6446(96)10028-3).
- [20] H. Goto, S. Yano, H. Zhang, Y. Matsumori, H. Ogawa, D.C. Blakey, S. Sone, Activity of a new vascular targeting agent, ZD6126, in pulmonary metastases by human lung adenocarcinoma in nude mice, *Cancer Res.* 62 (2002) 3711–3715.
- [21] J.W. Lippert, Vascular disrupting agents, *Bioorg. Med. Chem.* 15 (2007) 605–615. <https://doi.org/10.1016/j.bmc.2006.10.020>.
- [22] M. Cushman, D. Nagarathnam, D. Gopal, A.K. Chakraborti, C.M. Lin, E. Hamel, Synthesis and evaluation of stilbene and dihydrostilbene derivatives as potential anticancer agents that inhibit tubulin polymerization, *J. Med. Chem.* 34 (1991) 2579–2588. <https://doi.org/10.1021/jm00112a036>.
- [23] M. Cushman, D. Nagarathnam, D. Gopal, H.M. He, C.M. Lin, E. Hamel, Synthesis and evaluation of analogs of (Z)-1-(4-methoxyphenyl)-2-(3,4,5-trimethoxyphenyl)ethene as potential cytotoxic and antimetabolic agents, *J. Med. Chem.* 35 (1992) 2293–2306. <https://doi.org/10.1021/jm00090a021>.
- [24] K. Ohsumi, R. Nakagawa, Y. Fukuda, T. Hatanaka, Y. Morinaga, Y. Nihei, K. Ohishi, Y. Suga, Y. Akiyama, T. Tsuji, Novel Combretastatin Analogues Effective against Murine Solid Tumors: Design and Structure-Activity Relationships, *J. Med. Chem.* 41 (1998) 3022–3032. <https://doi.org/10.1021/jm980101w>.
- [25] N.H. Nam, Combretastatin A-4 Analogues as Antimetabolic Antitumor Agents, *Curr. Med. Chem.* 10 (2003) 1697–1722. <https://doi.org/10.2174/0929867033457151>.
- [26] M. Cushman, D. Nagarathnam, D. Gopal, H.M. He, C.M. Lin, E. Hamel, Synthesis and evaluation of analogues of (Z)-1-(4-methoxyphenyl)-2-(3,4,5-trimethoxyphenyl)ethene as potential cytotoxic and antimetabolic agents, *J. Med. Chem.* 35 (1992) 2293–2306.
- [27] K. Gaukroger, J.A. Hadfield, N.J. Lawrence, S. Nolan, A.T. McGown, Structural requirements for the interaction of combretastatins with tubulin: how important is the trimethoxy unit?, *Org. Biomol. Chem.* 1 (2003) 3033–3037. <https://doi.org/10.1039/B306878A>.
- [28] R. Romagnoli, P.G. Baraldi, M.K. Salvador, D. Preti, M. Aghazadeh Tabrizi, A. Brancale, X.H. Fu, J. Li, S.Z. Zhang, E. Hamel, R. Bortolozzi, G. Basso, G. Viola, Synthesis and Evaluation of 1,5-Disubstituted Tetrazoles as Rigid Analogues of Combretastatin A-4 with Potent Antiproliferative and Antitumor Activity, *J. Med. Chem.* 55 (2012) 475–488. <https://doi.org/10.1021/jm2013979>.
- [29] Data for in vitro cytotoxicity assay of combretastatin A-4, NCI database, internet website: <https://dtp.cancer.gov/dtpstandard/dwindex/index.jsp>, NSC 613729, (updated 6-2016), DTP 60 cell/5 dose data, GI50 Mean Graph of 6 Tests.

- [30] G.R. Pettit, B. Toki, D.L. Herald, P. Verdier-Pinard, M.R. Boyd, E. Hamel, R.K. Pettit, Antineoplastic agents. 379. Synthesis of phenstatin phosphate, *J. Med. Chem.* 41 (1998) 1688–1695. <https://doi.org/10.1021/jm970644q>.
- [31] S. Ducki, R. Forrest, J.A. Hadfield, A. Kendall, N.J. Lawrence, A.T. McGown, D. Rennison, Potent antimetabolic and cell growth inhibitory properties of substituted chalcones, *Bioorg. Med. Chem. Lett.* 8 (1998) 1051–1056.
- [32] L. Wang, K.W. Woods, Q. Li, K.J. Barr, R.W. McCroskey, S.M. Hannick, L. Gherke, R.B. Credo, Y.H. Hui, K. Marsh, R. Warner, J.Y. Lee, N. Zielinski-Mozng, D. Frost, S.H. Rosenberg, H.L. Sham, Potent, orally active heterocycle-based combretastatin A-4 analogues: synthesis, structure-activity relationship, pharmacokinetics, and *in vivo* antitumor activity evaluation, *J. Med. Chem.* 45 (2002) 1697–1711.
- [33] K. Mahal, B. Biersack, H. Caysa, R. Schobert, T. Mueller, Combretastatin A-4 derived imidazoles show cytotoxic, antivascular, and antimetastatic effects based on cytoskeletal reorganisation, *Invest. New Drugs.* 33 (2015) 541–554. <https://doi.org/10.1007/s10637-015-0215-9>.
- [34] A. Brancale, R. Silvestri, Indole, a core nucleus for potent inhibitors of tubulin polymerization, *Med. Res. Rev.* 27 (2007) 209–238. <https://doi.org/10.1002/med.20080>.
- [35] O.M. Aly, E.A. Beshr, R.M. Maklad, M. Mustafa, A.M. Gamal-Eldeen, Synthesis, Cytotoxicity, Docking Study, and Tubulin Polymerization Inhibitory Activity of Novel 1-(3,4-Dimethoxyphenyl)-5-(3,4,5-trimethoxyphenyl)-1*H*-1,2,4-triazole-3-carboxanilides: 1-(3,4-Dimethoxyphenyl)-5-(3,4,5-trimethoxyphenyl)-1*H*-1,2,4-triazole-3-carboxanilides, *Arch. Pharm. (Weinheim).* 347 (2014) 658–667. <https://doi.org/10.1002/ardp.201400096>.
- [36] J. Kaffy, R. Pontikis, J.C. Florent, C. Monneret, Synthesis and biological evaluation of vinylogous combretastatin A-4 derivatives, *Org. Biomol. Chem.* 3 (2005) 2657–2660. <https://doi.org/10.1039/b505955k>.
- [37] S. Aprile, E. Del Grosso, G.C. Tron, G. Grosa, *In Vitro* Metabolism Study of Combretastatin A-4 in Rat and Human Liver Microsomes, *Drug Metab. Dispos.* 35 (2007) 2252–2261. <https://doi.org/10.1124/dmd.107.016998>.
- [38] S. Thota, D.A. Rodrigues, P. de S.M. Pinheiro, L.M. Lima, C.A.M. Fraga, E.J. Barreiro, N-Acylhydrazones as drugs, *Bioorg. Med. Chem. Lett.* 28 (2018) 2797–2806. <https://doi.org/10.1016/j.bmcl.2018.07.015>.
- [39] R. do C. Maia, R. Tesch, C.A.M. Fraga, Acylhydrazone derivatives: a patent review, *Expert Opin. Ther. Pat.* 24 (2014) 1161–1170. <https://doi.org/10.1517/13543776.2014.959491>.
- [40] A. Sabt, O.M. Abdelhafez, R.S. El-Haggag, H.M.F. Madkour, W.M. Eldehna, E.E.-D.A.M. El-Khrisy, M.A. Abdel-Rahman, Laila.A. Rashed, Novel coumarin-6-sulfonamides as apoptotic anti-proliferative agents: synthesis, *in vitro* biological evaluation, and QSAR studies, *J. Enzyme Inhib. Med. Chem.* 33 (2018) 1095–1107. <https://doi.org/10.1080/14756366.2018.1477137>.
- [41] W.M. Eldehna, R.I. Al-Wabli, M.S. Almutairi, A.B. Keeton, G.A. Piazza, H.A. Abdel-Aziz, M.I. Attia, Synthesis and biological evaluation of certain hydrazonoindolin-2-one

- derivatives as new potent anti-proliferative agents, *J. Enzyme Inhib. Med. Chem.* 33 (2018) 867–878. <https://doi.org/10.1080/14756366.2018.1462802>.
- [42] N. Trotsko, A. Przekora, J. Zalewska, G. Ginalska, A. Paneth, M. Wujec, Synthesis and *in vitro* antiproliferative and antibacterial activity of new thiazolidine-2,4-dione derivatives, *J. Enzyme Inhib. Med. Chem.* 33 (2018) 17–24. <https://doi.org/10.1080/14756366.2017.1387543>.
- [43] D. Das Mukherjee, N.M. Kumar, M.P. Tantak, A. Das, A. Ganguli, S. Datta, D. Kumar, G. Chakrabarti, Development of Novel Bis(indolyl)-hydrazide–Hydrazone Derivatives as Potent Microtubule-Targeting Cytotoxic Agents against A549 Lung Cancer Cells, *Biochemistry.* 55 (2016) 3020–3035. <https://doi.org/10.1021/acs.biochem.5b01127>.
- [44] R. Sreenivasulu, K.T. Reddy, P. Sujitha, C.G. Kumar, R.R. Raju, Synthesis, antiproliferative and apoptosis induction potential activities of novel bis(indolyl)hydrazide-hydrazone derivatives, *Bioorg. Med. Chem.* 27 (2019) 1043–1055. <https://doi.org/10.1016/j.bmc.2019.02.002>.
- [45] M. de Freitas Silva, L.F. Coelho, I.M. Guirelli, R.M. Pereira, G.Á. Ferreira-Silva, G.Y. Graravelli, R. de O. Horvath, E.S. Caixeta, M. Ionta, C. Viegas, Synthetic resveratrol-curcumin hybrid derivative inhibits mitosis progression in estrogen positive MCF-7 breast cancer cells, *Toxicol. In Vitro.* 50 (2018) 75–85. <https://doi.org/10.1016/j.tiv.2018.02.020>.
- [46] H. He, X. Wang, L. Shi, W. Yin, Z. Yang, H. He, Y. Liang, Synthesis, antitumor activity and mechanism of action of novel 1,3-thiazole derivatives containing hydrazide–hydrazone and carboxamide moiety, *Bioorg. Med. Chem. Lett.* 26 (2016) 3263–3270. <https://doi.org/10.1016/j.bmcl.2016.05.059>.
- [47] B. Yadagiri, U.D. Holagunda, R. Bantu, L. Nagarapu, V. Guguloth, S. Polepally, N. Jain, Rational design, synthesis and anti-proliferative evaluation of novel benzosuberone tethered with hydrazide–hydrazones, *Bioorg. Med. Chem. Lett.* 24 (2014) 5041–5044. <https://doi.org/10.1016/j.bmcl.2014.09.018>.
- [48] D. Kumar, N. Maruthi Kumar, S. Ghosh, K. Shah, Novel bis(indolyl)hydrazide–hydrazones as potent cytotoxic agents, *Bioorg. Med. Chem. Lett.* 22 (2012) 212–215. <https://doi.org/10.1016/j.bmcl.2011.11.031>.
- [49] S. Vogel, D. Kaufmann, M. Pojarová, C. Müller, T. Pfaller, S. Kühne, P.J. Bednarski, E. von Angerer, Aroyl hydrazones of 2-phenylindole-3-carbaldehydes as novel antimetabolic agents, *Bioorg. Med. Chem.* 16 (2008) 6436–6447. <https://doi.org/10.1016/j.bmc.2008.04.071>.
- [50] H.-Z. Zhang, J. Drewe, B. Tseng, S. Kasibhatla, S.X. Cai, Discovery and SAR of indole-2-carboxylic acid benzylidene-hydrazides as a new series of potent apoptosis inducers using a cell-based HTS assay, *Bioorg. Med. Chem.* 12 (2004) 3649–3655. <https://doi.org/10.1016/j.bmc.2004.04.017>.
- [51] R. Sreenivasulu, R. Durgesh, S.S. Jadav, P. Sujitha, C. Ganesh Kumar, R.R. Raju, Synthesis, anticancer evaluation and molecular docking studies of bis(indolyl) triazinones,

- Nortopsentin analogs, *Chem. Pap.* 72 (2018) 1369–1378. <https://doi.org/10.1007/s11696-017-0372-8>.
- [52] S. Wang, H.Y. Liu, R.F. Xu, J. Sun, Synthesis, biological evaluation, and molecular docking studies of diacylhydrazine derivatives possessing 1,4-benzodioxan moiety as potential anticancer agents, *Russ. J. Gen. Chem.* 87 (2017) 2671–2677. <https://doi.org/10.1134/S1070363217110238>.
- [53] L.B. Salum, A. Mascarello, R.R. Canevarolo, W.F. Altei, A.B.A. Laranjeira, P.D. Neuenfeldt, T.R. Stumpf, L.D. Chiaradia-Delatorre, L.L. Vollmer, H.N. Daghestani, C.P. de Souza Melo, A.B. Silveira, P.C. Leal, M.J.S. Frederico, L.F. do Nascimento, A.R.S. Santos, A.D. Andricopulo, B.W. Day, R.A. Yunes, A. Vogt, J.A. Yunes, R.J. Nunes, N-(1'-naphthyl)-3,4,5-trimethoxybenzohydrazide as microtubule destabilizer: Synthesis, cytotoxicity, inhibition of cell migration and in vivo activity against acute lymphoblastic leukemia, *Eur. J. Med. Chem.* 96 (2015) 504–518. <https://doi.org/10.1016/j.ejmech.2015.02.041>.
- [54] M.P. Tantak, L. Klingler, V. Arun, A. Kumar, R. Sadana, D. Kumar, Design and synthesis of bis(indolyl)ketohydrazide-hydrazones: Identification of potent and selective novel tubulin inhibitors, *Eur. J. Med. Chem.* 136 (2017) 184–194. <https://doi.org/10.1016/j.ejmech.2017.04.078>.
- [55] G. Bacher, B. Nickel, P. Emig, U. Vanhoefer, S. Seeber, A. Shandra, T. Klenner, T. Beckers, D-24851, a novel synthetic microtubule inhibitor, exerts curative antitumoral activity in vivo, shows efficacy toward multidrug-resistant tumor cells, and lacks neurotoxicity, *Cancer Res.* 61 (2001) 392–399.
- [56] B. Burja, T. Čimbora-Zovko, S. Tomić, T. Jelušić, M. Kočevar, S. Polanc, M. Osmak, Pyrazolone-fused combretastatins and their precursors: synthesis, cytotoxicity, antitubulin activity and molecular modeling studies, *Bioorg. Med. Chem.* 18 (2010) 2375–2387. <https://doi.org/10.1016/j.bmc.2010.03.006>.
- [57] B.G. Szczepankiewicz, G. Liu, H.S. Jae, A.S. Tasker, I.W. Gunawardana, T.W. von Geldern, S.L. Gwaltney, J.R. Wu-Wong, L. Gehrke, W.J. Chiou, R.B. Credo, J.D. Alder, M.A. Nukkala, N.A. Zielinski, K. Jarvis, K.W. Mollison, D.J. Frost, J.L. Bauch, Y.H. Hui, A.K. Claiborne, Q. Li, S.H. Rosenberg, New Antimitotic Agents with Activity in Multi-Drug-Resistant Cell Lines and in Vivo Efficacy in Murine Tumor Models, *J. Med. Chem.* 44 (2001) 4416–4430. <https://doi.org/10.1021/jm010231w>.
- [58] Y. Hu, C.Y. Li, X.M. Wang, Y.H. Yang, H.L. Zhu, 1,3,4-Thiadiazole: Synthesis, Reactions, and Applications in Medicinal, Agricultural, and Materials Chemistry, *Chem. Rev.* 114 (2014) 5572–5610. <https://doi.org/10.1021/cr400131u>.
- [59] D. Kumar, N. Maruthi Kumar, K.H. Chang, K. Shah, Synthesis and anticancer activity of 5-(3-indolyl)-1,3,4-thiadiazoles, *Eur. J. Med. Chem.* 45 (2010) 4664–4668. <https://doi.org/10.1016/j.ejmech.2010.07.023>.
- [60] A. Kamal, D. Dastagiri, M.J. Ramaiah, E.V. Bharathi, J.S. Reddy, G. Balakishan, P. Sarma, S.N.C.V.L. Pushpavalli, M. Pal-Bhadra, A. Juvekar, S. Sen, S. Zingde, Synthesis,

- anticancer activity and mitochondrial mediated apoptosis inducing ability of 2,5-diaryloxadiazole-pyrrolobenzodiazepine conjugates, *Bioorg. Med. Chem.* 18 (2010) 6666–6677. <https://doi.org/10.1016/j.bmc.2010.07.067>.
- [61] N. Sirisoma, A. Pervin, J. Drewe, B. Tseng, S.X. Cai, Discovery of substituted N'-(2-oxoindolin-3-ylidene)benzohydrazides as new apoptosis inducers using a cell- and caspase-based HTS assay, *Bioorg. Med. Chem. Lett.* 19 (2009) 2710–2713. <https://doi.org/10.1016/j.bmcl.2009.03.121>.
- [62] R.B.G. Ravelli, B. Gigant, P.A. Curmi, I. Jourdain, S. Lachkar, A. Sobel, M. Knossow, Insight into tubulin regulation from a complex with colchicine and a stathmin-like domain, *Nature*. 428 (2004) 198–202. <https://doi.org/10.1038/nature02393>.
- [63] J. Marangon, M.S. Christodoulou, F.V.M. Casagrande, G. Tiana, L. Dalla Via, A. Aliverti, D. Passarella, G. Cappelletti, S. Ricagno, Tools for the rational design of bivalent microtubule-targeting drugs, *Biochem. Biophys. Res. Commun.* 479 (2016) 48–53. <https://doi.org/10.1016/j.bbrc.2016.09.022>.
- [64] A.E. Prota, F. Danel, F. Bachmann, K. Bargsten, R.M. Buey, J. Pohlmann, S. Reinelt, H. Lane, M.O. Steinmetz, The novel microtubule-destabilizing drug BAL27862 binds to the colchicine site of tubulin with distinct effects on microtubule organization, *J. Mol. Biol.* 426 (2014) 1848–1860. <https://doi.org/10.1016/j.jmb.2014.02.005>.
- [65] P. Zhou, Y. Liu, L. Zhou, K. Zhu, K. Feng, H. Zhang, Y. Liang, H. Jiang, C. Luo, M. Liu, Y. Wang, Potent Antitumor Activities and Structure Basis of the Chiral β -Lactam Bridged Analogue of Combretastatin A-4 Binding to Tubulin, *J. Med. Chem.* 59 (2016) 10329–10334. <https://doi.org/10.1021/acs.jmedchem.6b01268>.
- [66] M.D. Canela, S. Noppen, O. Bueno, A.E. Prota, K. Bargsten, G. Sáez-Calvo, M.L. Jimeno, M. Benkheil, D. Ribatti, S. Velázquez, M.J. Camarasa, J.F. Díaz, M.O. Steinmetz, E.M. Priego, M.J. Pérez-Pérez, S. Liekens, Antivascular and antitumor properties of the tubulin-binding chalcone TUB091, *Oncotarget*. 8 (2017) 14325–14342. <https://doi.org/10.18632/oncotarget.9527>.
- [67] R. Gaspari, A.E. Prota, K. Bargsten, A. Cavalli, M.O. Steinmetz, Structural Basis of cis - and trans -Combretastatin Binding to Tubulin, *Chem.* 2 (2017) 102–113. <https://doi.org/10.1016/j.chempr.2016.12.005>.
- [68] S.L. Dixon, A.M. Smondyrev, S.N. Rao, PHASE: A Novel Approach to Pharmacophore Modeling and 3D Database Searching, *Chem. Biol. Drug Des.* 67 (2006) 370–372. <https://doi.org/10.1111/j.1747-0285.2006.00384.x>.
- [69] Maestro, version 9.0, Schrödinger, LLC, New York, USA, 2009. www.schrodinger.com.
- [70] M.P. Jacobson, D.L. Pincus, C.S. Rapp, T.J.F. Day, B. Honig, D.E. Shaw, R.A. Friesner, A hierarchical approach to all-atom protein loop prediction, *Proteins*. 55 (2004) 351–367. <https://doi.org/10.1002/prot.10613>.
- [71] D.E. Koshland, Application of a Theory of Enzyme Specificity to Protein Synthesis, *Proc. Natl. Acad. Sci. U. S. A.* 44 (1958) 98–104.

- [72] F. Mauthner, Trimethylgallic Acid, *Org. Synth.* 6 (1926) 96, (Checked by H. T. Clarke). <https://doi.org/10.15227/orgsyn.006.0096>.
- [73] A.S. Chida, P.V.S.N. Vani, M. Chandrasekharam, R. Srinivasan, A.K. Singh, Synthesis of 2,3-Dimethoxy-5-methyl-1,4-benzoquinone: A Key Fragment in Coenzyme-Q Series *, *Synth. Commun.* 31 (2001) 657–660. <https://doi.org/10.1081/SCC-100103252>.
- [74] S. Zuffanti, Preparation of acyl chlorides with thionyl chloride., *J. Chem. Educ.* 25 (1948) 481. <https://doi.org/10.1021/ed025p481>.
- [75] Data of the commercially available 4-allyloxybenzoyl chloride is found under CAS (Chemical Abstract Service) Number 36844-51-6.
- [76] Data of the commercially available 4-methoxy-3-nitrobenzoyl chloride is found under CAS (Chemical Abstract Service) Number 10397-28-1.
- [77] Data of the commercially available 4-methoxybenzoyl chloride (p-anisoyl chloride) is found under CAS (Chemical Abstract Service) Number 100-07-2.
- [78] J. Li, C. Yang, Y. Bai, X. Yang, Y. Liu, J. Peng, The effect of an acylphosphine ligand on the rhodium-catalyzed hydrosilylation of alkenes, *J. Organomet. Chem.* 855 (2018) 7–11. <https://doi.org/10.1016/j.jorganchem.2017.12.004>.
- [79] Data of the commercially available 3-chloro-4-ethoxybenzoyl chloride is found under CAS (Chemical Abstract Service) Number 81324-60-9.
- [80] A.A. Kanhed, A.P. Mehre, K.R. Pandey, D.K. Mahapatra, 4-(2-Chloroacetamido) Benzoic Acid Derivatives as Local Anesthetic Agents: Design, Synthesis, and Characterization, *UK J. Pharm. Biosci.* 4 (2016) 35. <https://doi.org/10.20510/ukjpb/4/i6/134659>.
- [81] C.C. Chen, C.H. Lin, Synthesis and Characterization of Liquid Crystalline Organosiloxanes Containing 4-Methoxyphenyl 4-(2-alkenyloxy)benzoate, *Asian J. Chem.* 28 (2016) 1270–1274. <https://doi.org/10.14233/ajchem.2016.19651>.
- [82] R. Ueno, M. Kitayama, H. Wakamori, Process for producing 3-nitro-4-alkoxybenzoic acid, WO/2004/096750, 2004.
- [83] Z. Zhang, Y. Yi, J. Liu, Method for preparing 3-nitro-4-methoxy benzoic acid, CN 104356000, 2015.
- [84] Data of the commercially available 4-methoxybenzoic acid is found under CAS (Chemical Abstract Service) Number 100-09-4.
- [85] Data of the commercially available 3-chloro-4-ethoxybenzoic acid is found under CAS (Chemical Abstract Service) Number 213598-15-3.
- [86] B. Bhatia, J. Iqbal, Cobalt (II) catalyzed oxidation of aldehydes to carboxylic acid with molecular oxygen, *Tetrahedron Lett.* 33 (1992) 7961–7964. [https://doi.org/10.1016/S0040-4039\(00\)74789-7](https://doi.org/10.1016/S0040-4039(00)74789-7).
- [87] K. Kar, U. Krithika, Mithuna, P. Basu, S. Santhosh Kumar, A. Reji, B.R. Prashantha Kumar, Design, synthesis and glucose uptake activity of some novel glitazones, *Bioorganic Chem.* 56 (2014) 27–33. <https://doi.org/10.1016/j.bioorg.2014.05.006>.
- [88] N.P. Rai, V.K. Narayanaswamy, S. Shashikanth, P.N. Arunachalam, Synthesis, characterization and antibacterial activity of 2-[1-(5-chloro-2-methoxy-phenyl)-5-methyl-

- 1H-pyrazol-4-yl]-5-(substituted-phenyl)-[1,3,4]oxadiazoles, *Eur. J. Med. Chem.* 44 (2009) 4522–4527. <https://doi.org/10.1016/j.ejmech.2009.06.020>.
- [89] P. Majumdar, A. Pati, M. Patra, R.K. Behera, A.K. Behera, Acid Hydrazides, Potent Reagents for Synthesis of Oxygen-, Nitrogen-, and/or Sulfur-Containing Heterocyclic Rings, *Chem. Rev.* 114 (2014) 2942–2977. <https://doi.org/10.1021/cr300122t>.
- [90] V.V. Semenov, A.S. Kiselyov, I.Y. Titov, I.K. Sagamanova, N.N. Ikizalp, N.B. Chernysheva, D.V. Tsyganov, L.D. Konyushkin, S.I. Firgang, R.V. Semenov, I.B. Karmanova, M.M. Raihstat, M.N. Semenova, Synthesis of Antimitotic Polyalkoxyphenyl Derivatives of Combretastatin Using Plant Allylpolyalkoxybenzenes(1), *J. Nat. Prod.* 73 (2010) 1796–1802. <https://doi.org/10.1021/np1004278>.
- [91] Data for in vitro cytotoxicity assay of colchicine, NCI database, internet website: <https://dtp.cancer.gov/dtpstandard/dwindex/index.jsp>, NSC 757, updated 6-2016, One-dose data graph.
- [92] T. Mosmann, Rapid colorimetric assay for cellular growth and survival: application to proliferation and cytotoxicity assays, *J. Immunol. Methods.* 65 (1983) 55–63.
- [93] D.A. Scudiero, R.H. Shoemaker, K.D. Paull, A. Monks, S. Tierney, T.H. Nofziger, M.J. Currens, D. Seniff, M.R. Boyd, Evaluation of a soluble tetrazolium/formazan assay for cell growth and drug sensitivity in culture using human and other tumor cell lines, *Cancer Res.* 48 (1988) 4827–4833.
- [94] W.M. Eldehna, D.H. EL-Naggar, A.R. Hamed, H.S. Ibrahim, H.A. Ghabbour, H.A. Abdel-Aziz, One-pot three-component synthesis of novel spirooxindoles with potential cytotoxic activity against triple-negative breast cancer MDA-MB-231 cells, *J. Enzyme Inhib. Med. Chem.* 33 (2018) 309–318. <https://doi.org/10.1080/14756366.2017.1417276>.
- [95] G. Zhang, V. Gurtu, S.R. Kain, G. Yan, Early Detection of Apoptosis Using a Fluorescent Conjugate of Annexin V, *BioTechniques.* 23 (1997) 525–531. <https://doi.org/10.2144/97233pf01>.
- [96] H. Lecoer, Nuclear Apoptosis Detection by Flow Cytometry: Influence of Endogenous Endonucleases, *Exp. Cell Res.* 277 (2002) 1–14. <https://doi.org/10.1006/excr.2002.5537>.
- [97] M. Szumilak, A. Szulawska-Mroczek, K. Koprowska, M. Stasiak, W. Lewgowd, A. Stanczak, M. Czyz, Synthesis and in vitro biological evaluation of new polyamine conjugates as potential anticancer drugs, *Eur. J. Med. Chem.* 45 (2010) 5744–5751. <https://doi.org/10.1016/j.ejmech.2010.09.032>.
- [98] C.H. Reynolds, R.E. Hormann, Theoretical Study of the Structure and Rotational Flexibility of Diacylhydrazines: Implications for the Structure of Nonsteroidal Ecdysone Agonists and Azapeptides, *J. Am. Chem. Soc.* 118 (1996) 9395–9401. <https://doi.org/10.1021/ja960214+>.
- [99] R. Romagnoli, P.G. Baraldi, O. Cruz-Lopez, C. Lopez Cara, M.D. Carrion, A. Brancale, E. Hamel, L. Chen, R. Bortolozzi, G. Basso, G. Viola, Synthesis and Antitumor Activity of 1,5-Disubstituted 1,2,4-Triazoles as Cis-Restricted Combretastatin Analogues, *J. Med. Chem.* 53 (2010) 4248–4258. <https://doi.org/10.1021/jm100245q>.

- [100] J.R. Wu-Wong, J.D. Alder, L. Alder, D.J. Burns, E.K. Han, B. Credo, S.K. Tahir, B.D. Dayton, P.J. Ewing, W.J. Chiou, Identification and characterization of A-105972, an antineoplastic agent, *Cancer Res.* 61 (2001) 1486–1492.
- [101] L. Lee, L.M. Robb, M. Lee, R. Davis, H. Mackay, S. Chavda, B. Babu, E.L. O'Brien, A.L. Risinger, S.L. Mooberry, M. Lee, Design, Synthesis, and Biological Evaluations of 2,5-Diaryl-2,3-dihydro-1,3,4-oxadiazoline Analogs of Combretastatin-A4, *J. Med. Chem.* 53 (2010) 325–334. <https://doi.org/10.1021/jm901268n>.
- [102] C.M. Sun, L.G. Lin, H.J. Yu, C.Y. Cheng, Y.C. Tsai, C.W. Chu, Y.H. Din, Y.P. Chau, M.J. Don, Synthesis and cytotoxic activities of 4,5-diarylisoaxazoles, *Bioorg. Med. Chem. Lett.* 17 (2007) 1078–1081. <https://doi.org/10.1016/j.bmcl.2006.11.023>.
- [103] R. Bai, X.F. Pei, O. Boyé, Z. Getahun, S. Grover, J. Bekisz, N.Y. Nguyen, A. Brossi, E. Hamel, Identification of Cysteine 354 of β -Tubulin as Part of the Binding Site for the A Ring of Colchicine, *J. Biol. Chem.* 271 (1996) 12639–12645. <https://doi.org/10.1074/jbc.271.21.12639>.
- [104] R. Bai, D.G. Covell, X.F. Pei, J.B. Ewell, N.Y. Nguyen, A. Brossi, E. Hamel, Mapping the Binding Site of Colchicinoids on β -Tubulin: 2-Chloroacetyl-2-demethylthiocolchicine Covalently Reacts Predominantly with Cysteine 239 and Secondarily with Cysteine 354, *J. Biol. Chem.* 275 (2000) 40443–40452. <https://doi.org/10.1074/jbc.M005299200>.
- [105] I. Zaki, M.K. Abdelhameid, I.M. El-Deen, A.H.A. Abdel Wahab, A.M. Ashmawy, K.O. Mohamed, Design, synthesis and screening of 1, 2, 4-triazinone derivatives as potential antitumor agents with apoptosis inducing activity on MCF-7 breast cancer cell line, *Eur. J. Med. Chem.* 156 (2018) 563–579. <https://doi.org/10.1016/j.ejmech.2018.07.003>.

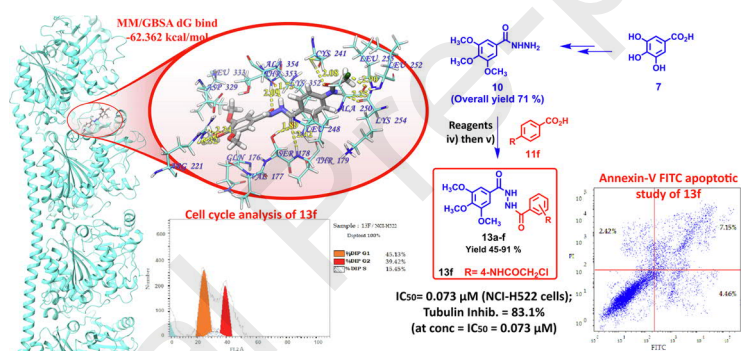
Declaration of interests

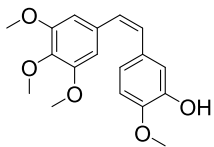
The authors declare that they have no known competing financial interests or personal relationships that could have appeared to influence the work reported in this paper.

The authors declare the following financial interests/personal relationships which may be considered as potential competing interests:

Highlights:

- *Bis*-hydrazide CA-4 analogues **13a-h** were designed and synthesized with modified ring B.
- Docking study inside flexible receptor revealed maximal binding energy for **13f**-tubulin complex.
- Compound **13f** displayed 34% death in NCI-H522 cells at 10 μ M in NCI-60 cell line assay.
- Compound **13f** displayed IC₅₀ of 0.073 μ M (MTT assay) & 83.1% tubulin inhibition in NCI-H522 cells.
- At its IC₅₀, **13f** induced cell cycle arrest at G2/M phase & 11.6% apoptosis at preG1 phase.

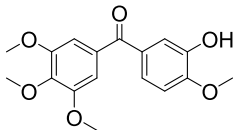




1 (CA-4)

IC₅₀ (Hela Cells) [28] = 4 nM
 IC₅₀ (Colon 26 cells) [24] = 18 nM
 IC₅₀ (OVCAR-3 cells) [29]^a = 39.8 nM
 IC₅₀ (HCT116 cells) [35] = 16 nM
 IC₅₀ (K562 cells) [31] = 31.6 nM

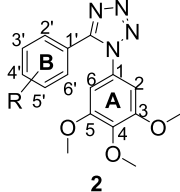
Tubulin Inhib. IC₅₀ [28] = 1.3 μM
 [24] = 4 μM
 [35] = 1.2 μM



4 (Phenstatin)

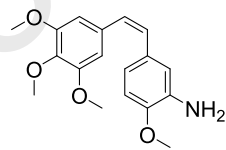
IC₅₀ (OVCAR-3 cells) [30] = 7.22 nM

Tubulin Inhib.
 IC₅₀ [30] = 1.2 μM



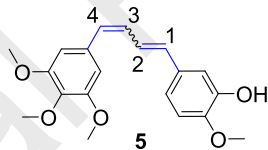
2

| R= | IC ₅₀ (nM) Hela cells [28] | Tubulin Inhib. IC ₅₀ (μM) [28] |
|------------------------|--|--|
| 2a 4'-OMe | 2.6 | 2.5 |
| 2b 4'-OEt | 1.9 | 1.1 |
| 2c 4'-O-n-Pr | 2.6 | 3.1 |
| 2d 4'-O-n-Bu | 11.1 | ND ^b |
| 2e 4'-O-pentyl | >10000 | ND |
| 2f 3'-Cl,4'-OMe | 2.3 | 3.5 |
| 2g 3'-Cl,4'-OEt | 2.6 | 2.0 |



3 (AC7700)

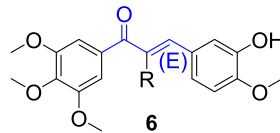
IC₅₀ (Colon 26 cells) [24] = 5.1 nM
 Tubulin Inhib. IC₅₀ [24] = 4 μM



5

IC₅₀ (nM) [35]
 (HCT116 cells) Tubulin Inhib.
 IC₅₀ (μM) [35]

| | | |
|--------------------------|-----|-----|
| 5a (1E,3Z) isomer | 163 | 2.3 |
| 5b (1Z,3E) isomer | 62 | 2.0 |



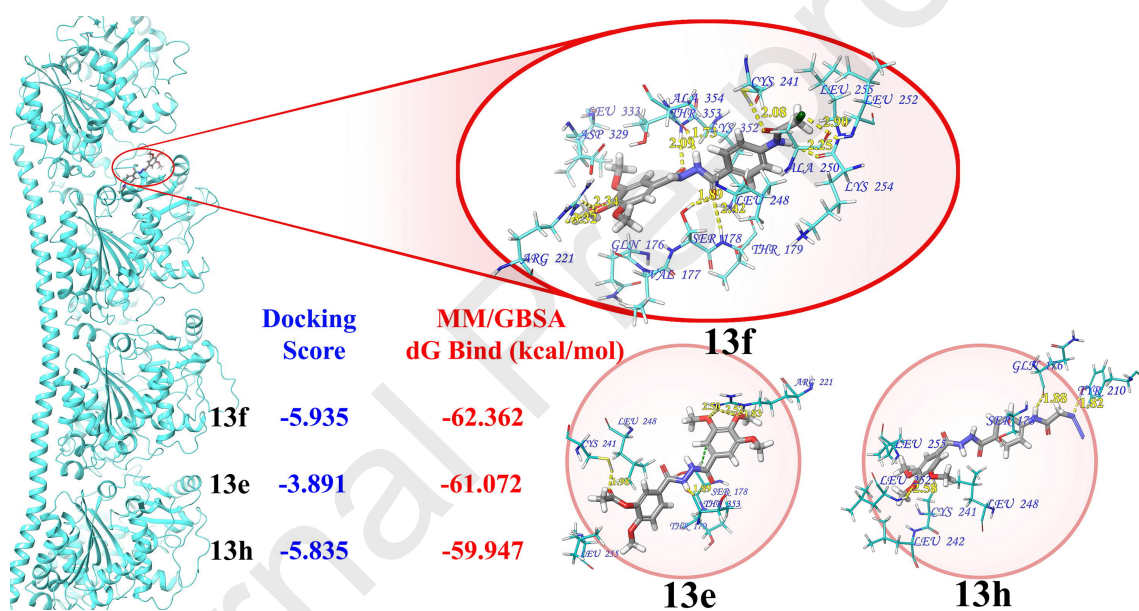
6

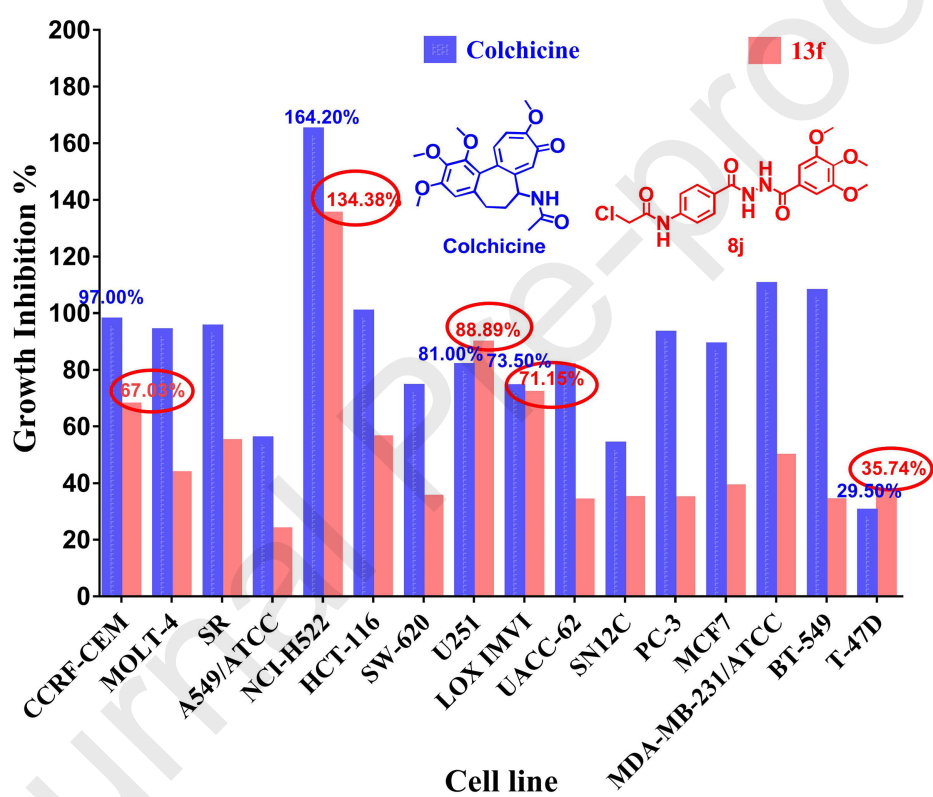
R IC₅₀ (nM) [31]
 (K562 cells) Tubulin Inhib.
 IC₅₀ (μM) [31]

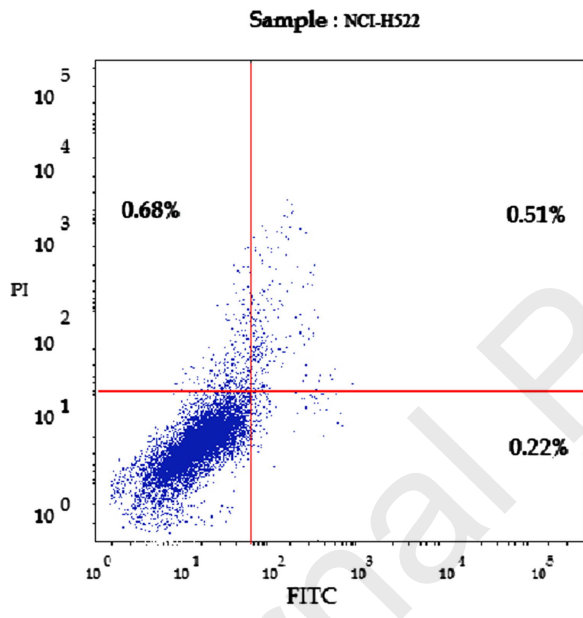
| | | |
|---------------------------|------|----|
| 6a H | 4.3 | ND |
| 6b CH ₃ | 0.21 | ND |

^a IC₅₀ data of CA-4 against OVCAR-3 cells was obtained from the five-dose GI₅₀ mean graph of CA-4, National Institute of Cancer (NCI) database (updated 24-1-2017)

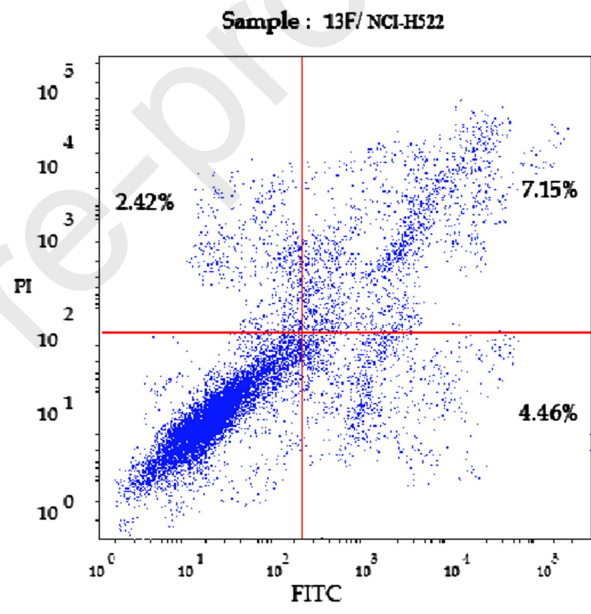
^b ND not determined.



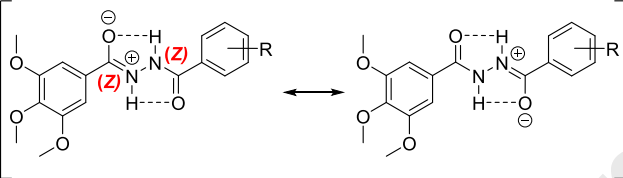




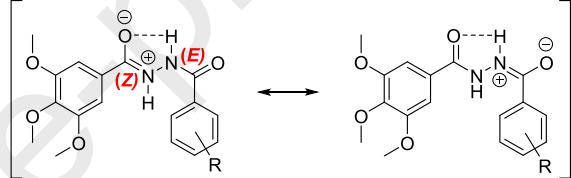
(a)



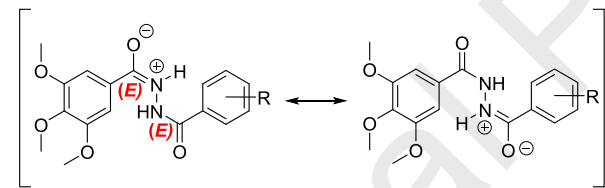
(b)



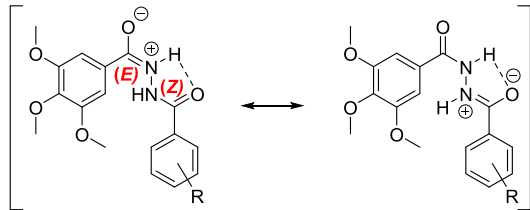
(Z,Z)-Conformer



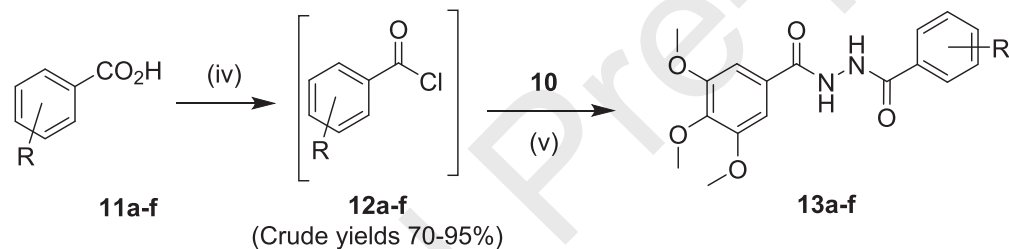
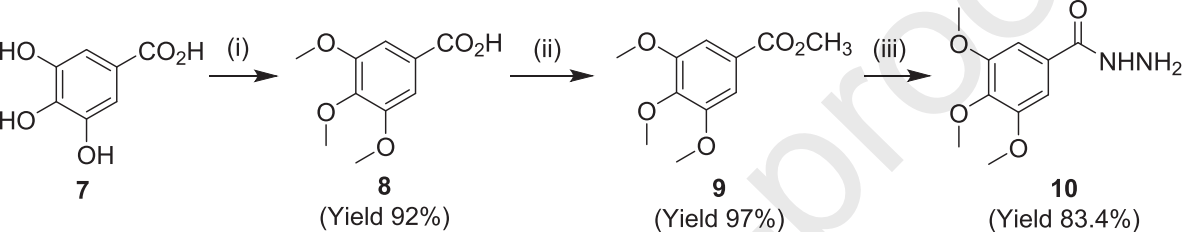
(Z,E)-Conformer



(E,E)-Conformer



(E,Z)-Conformer



| | | | | | |
|------------|------------|------------|--|------------|---------------|
| 11a | 12a | 13a | R= 4-O-allyl | 13a | (Yield 91.4%) |
| 11b | 12b | 13b | 3-NO ₂ , 4-OCH ₃ | 13b | (Yield 76.3%) |
| 11c | 12c | 13c | 4-OCH ₃ | 13c | (Yield 53%) |
| 11d | 12d | 13d | 3-Cl, 4-OEt | 13d | (Yield 48%) |
| 11e | 12e | 13e | 3-OAc, 4-OCH ₃ | 13e | (Yield 46%) |
| 11f | 12f | 13f | 4-NH-CO-CH ₂ Cl | 13f | (Yield 45%) |
| | | 13g | 3-OH, 4-OCH ₃ | 13g | (Yield 44%) |
| | | 13h | 4-NH-CO-CH ₂ N ₃ | 13h | (Yield 44%) |

(vi)

(vii)